HEI HEALTH EFFECTS INSTITUTE

Consequences of Prolonged Inhalation of Ozone on F344/N Rats: Collaborative Studies

Part XIII. A Comparison of Changes in the Tracheobronchial Epithelium and Pulmonary Acinus in Male Rats at 3 and 20 Months

Kent E. Pinkerton, Barbara L. Weller,
Margaret G. Ménache, and Charles G. Plopper
University of California, Davis, CA, Duke University, Durham, NC

Includes the Commentary of the Institute's Health Review Committee

Research Report Number 65
June 1998

HEI HEALTH EFFECTS INSTITUTE

The Health Effects Institute, established in 1980, is an independent and unbiased source of information on the health effects of motor vehicle emissions. HEI studies all major pollutants, including regulated pollutants (such as carbon monoxide, ozone, nitrogen dioxide, and particulate materials), and unregulated pollutants (such as diesel engine exhaust, methanol, and aldehydes). To date, HEI has supported more than 170 projects at institutions in North America and Europe.

Typically, HEI receives half its funds from the U.S. Environmental Protection Agency and half from 28 manufacturers and marketers of motor vehicles and engines in the United States. Occasionally, funds from other public or private organizations either support special projects or provide resources for a portion of an HEI study. For this study, the Institute acknowledges the cooperation and support of the National Toxicology Program (NTP), which consists of four charter agencies of the U.S. Department of Health and Human Services. The NTP sponsored a portion of the inhalation component of this project as part of its studies on the toxicologic and carcinogenic effects of ozone. Regardless of funding sources, HEI exercises complete autonomy in setting its research priorities and in reaching its conclusions. An independent Board of Directors governs HEI. The Institute's Research and Review Committees serve complementary scientific purposes and draw distinguished scientists as members. The results of HEI-funded studies are made available as Research Reports, which contain both the Investigators' Report and the Review Committee's evaluation of the work's scientific quality and regulatory relevance.

HEI Statement

Synopsis of Research Report Number 65 Part XIII

Changes in Lung Structure and Enzyme Activities in Rats Exposed to Ozone for Different Time Periods

BACKGROUND

Ozone, a common outdoor air pollutant, is a highly reactive gas and a major component of smog. Because ozone can damage cells, prolonged or repeated exposures could be a risk factor for cancer. For this reason, the National Toxicology Program (NTP) evaluated ozone's carcinogenicity in rodents. Another public health concern is that prolonged exposure to ozone might damage the airways and contribute to the development of noncancerous respiratory diseases. To examine this issue, the Health Effects Institute collaborated with the NTP to provide HEI-funded investigators access to animals that underwent the same rigorously controlled ozone exposure and quality assurance processes along with the animals used for NTP studies. In the NTP/HEI Collaborative Ozone Project, male and female F344/N rats were exposed to 0, 0.12, 0.5, or 1.0 ppm ozone for six hours per day, five days per week, for 20 months.

One of the NTP/HEI investigator groups, Dr. Kent Pinkerton and colleagues, conducted detailed analyses of ozone's effects on the cellular structure of the airways and lungs. They also studied the activity levels of antioxidant enzymes, which protect tissues against the potentially harmful effects of oxidants such as ozone. They observed cellular changes in the centriacinar region (the junction of the conducting airways and the gas exchange region of the lung) of rats exposed to 0.5 or 1.0 ppm ozone. Thin, ozone-sensitive epithelial cells normally lining this region were replaced by thicker, ozone-resistant epithelial cells that are more characteristic of the epithelium of bronchioles. Thickening of the interstitium, which supports the epithelium, also was seen in the alveolar ducts of rats exposed to 0.5 or 1.0 ppm ozone. These changes were accompanied by increased antioxidant enzyme activity in the small bronchioles. The investigators hypothesized that these changes may protect the centriacinar region from injury. However, because measurements were made only after 20 months of exposure in the NTP/HEI collaboration, the investigators could not determine when these changes occurred, whether changes earlier in the exposure period differed from those after 20 months of exposure, or whether aging affected the results.

APPROACH

Pinkerton and colleagues exposed male rats to 0, 0.12, or 1.0 ppm ozone for 2 or 3 months under conditions that closely replicated the original NTP exposure protocol. They conducted sophisticated structural and chemical analyses on airway tissues using techniques similar to those developed for their NTP/HEI study. They compared the results of this study with those obtained from male rats exposed to the same levels of ozone for 20 months.

RESULTS AND IMPLICATIONS

This study revealed two key findings. First, structural changes in the centriacinar region were seen after 2 or 3 months of exposure to 1.0 ppm ozone (but not to 0.12 ppm ozone) and the degree of these changes was similar to that seen after the 20-month ozone exposure. Thus, these ozone-induced changes do not appear to have been affected by aging. Second, the increase in antioxidant enzyme activity reported in their NTP/HEI study could be accounted for by an increase in the antioxidant enzyme superoxide dismutase in its manganese form. Taken together, the results indicate that the cellular and antioxidant enzyme changes previously observed in response to prolonged exposure to ozone occur early and are stable throughout a long exposure period. Accordingly, the early responses to ozone may represent changes that protect the rat lungs during continued exposure to ozone. However, it is not known whether these alterations to the anatomy of the centriacinar region are detrimental to lung health over the long term.

This Statement, prepared by the Health Effects Institute and approved by its Board of Directors, is a summary of a research project sponsored by HEI from 1995 to 1996. This study was conducted by Dr. Kent E. Pinkerton of the University of California, Davis, CA. The following Research Report contains both the detailed Investigators' Report and a Commentary on the study prepared by the Institute's Health Review Committee.

Library of Congress Catalog Number for the HEI Research Report Series: WA 754 R432.
The paper in this publication meets the minimum standard requirements of the ANSI Standard Z39.48-1984 (Permanence of Paper) effective with Report Number 21, December 1988, and with Report Numbers 25, 26, 32, 51, and 65 Parts IV, VIII, and IX excepted. These excepted Reports are printed on acid-free coated paper.

TABLE OF CONTENTS

Research Report Number 65 Part XIII

Consequences of Prolonged Inhalation of Ozone on F344/N Rats: Collaborative Studies Part XIII: A Comparison of Changes in the Tracheobronchial Epithelium and Pulmonary Acinus in Male Rats at 3 and 20 Months

Kent E. Pinkerton, Barbara L. Weller, Margaret G. Ménache, and Charles G. Plopper

Consequences of Prolonged Inhalation of Ozone on F344/N Rats: Collaborative Studies

Part XIII. A Comparison of Changes in the Tracheobronchial Epithelium and Pulmonary Acinus in Male Rats at 3 and 20 Months

Kent E. Pinkerton, Barbara L. Weller, Margaret G. Ménache, and Charles G. Plopper

ABSTRACT

A limitation of the NTP/HEI Collaborative Ozone Project conducted with F344/N rats at the Battelle Pacific Northwest Laboratories in Richland, WA (1991–1993) was that the study used only one time point (20 months) to examine the chronic effects of exposure to ozone. Issues the design of that study could not address were (1) the status of cellular differentiation at earlier time points during the course of ozone exposure; (2) whether changes that appeared to be compensatory after 20 months of exposure were due to ozone, or were aspects of the natural aging process in rats; (3) the inability to define adequately which effects were related specifically to the prolonged duration of exposure; and (4) how and what changes brought about by the natural aging process may have overridden or confounded a clear definition of the effects of exposure to ozone at ambient concentrations (e.g., 0.12 parts per million [ppm]*), which are of most concern with long-term exposure to this pollutant. The present study examined the effects of a 3-month exposure to ozone under conditions identical to those of the 20-month NTP/HEI Collaborative Ozone Project. In our facilities at the University of California, Davis, we exposed 42 male F344/N rats to either filtered air or 0.12 or 1.0 ppm ozone.

After 3 months of exposure to 1.0 ppm ozone, changes in the distribution of superoxide dismutase (SOD) in the copper-zinc (Cu-Zn) form were shown by a pattern of reduced staining in terminal bronchioles and the centriacinar region; and the manganese (Mn) form of SOD was elevated within the centriacinar region. Further analysis by transmission electron microscopy and immunogold labeling confirmed that Mn SOD was elevated within epithelial type II cells immediately distal to the bronchiole-alveolar duct junction (BADJ).

The trachea, three major bronchi, and a short-length and long-length airway path relative to the trachea were examined by morphometric techniques. The pulmonary acini arising from each of these two paths were also examined morphometrically as a function of distance into the alveolar duct. Cellular changes occurring in each of these anatomical regions after 3 months of exposure were analyzed and compared to the changes noted after the 20-month ozone exposures. We found significant increases in the volume density of nonciliated epithelial cells lining the trachea and caudal bronchi as well as in the proximal and terminal bronchioles of the cranial region at a concentration of 1.0 ppm ozone after both 3 and 20 months of exposure. Remodeling of the centriacinar region, particularly within the cranial region of the lungs after exposure to 1.0 ppm ozone, was statistically significant at both 3 and 20 months. No statistically significant effects were noted following exposure to 0.12 ppm ozone for either 3 or 20 months. An important finding was that age did not influence the effect of ozone on the lungs of rats. We conclude that long-term exposure to ozone, rather than the effects of aging, lead to significant alterations of epithelial cell populations lining the airways and centriacinar region of the lung. Marked cellular changes were noted after exposure to 1.0 ppm ozone, but not to 0.12 ppm.

INTRODUCTION

Modeling studies have predicted that the major sites for inhaled ozone uptake and reactivity are the anterior nasal cavity, the trachea, and the central acinus (Miller et al.

* A list of abbreviations appears at the end of the Investigators' Report.

This Investigators' Report is one section of Health Effects Institute Research Report Number 65 Part XIII, which also includes a Commentary by the Health Review Committee, and an HEI Statement about the research project. Correspondence concerning the Investigators' Report may be addressed to Dr. Kent E. Pinkerton, Institute of Toxicology and Environmental Health, School of Veterinary Medicine, University of California, Davis, CA 95616.

Although this document was produced with partial funding by the United States Environmental Protection Agency under Assistance Award R824835 to the Health Effects Institute, it has not been subjected to the Agency's peer and administrative review and therefore may not necessarily reflect the views of the Agency, and no official endorsement by it should be inferred. The contents of this document also have not been reviewed by private party institutions, including those that support the Health Effects Institute; therefore, it may not reflect the views or policies of these parties, and no endorsement by them should be inferred.

1985; Patra et al. 1986). The principal sites of injury within the lower respiratory tract after short-term ozone exposure are in the epithelium of the trachea and the centriacinar region, which includes the most distal bronchioles and the most proximal portion of the acinus (Dungworth et al. 1975; Barry et al. 1985; Nikula et al. 1988). By ultrastructural assessment, little or no injury has been detected in any of the intrapulmonary bronchi between the trachea and distal bronchioles, nor in at least 90% of the pulmonary acinus more distal than the centriacinar region (Boorman et al. 1980).

The nature of the pulmonary epithelial injury appears to be related to species, specific anatomic site, the composition of the epithelium before exposure, the concentration of ozone inhaled, and the duration of exposure up to about 3 months (described as: short-term, 3 days or less; intermediate, 7 to 10 days; and long-term, 60 days or longer) (Dungworth et al. 1975; Barry et al. 1985). (Note that the NTP/HEI Collaborative Ozone Project used "prolonged" to describe the 20-month exposure.) However, one intriguing characteristic of the pulmonary response to ozone is that the epithelial cell populations in target zones injured acutely by certain concentrations of ozone become resistant to those same concentrations when ozone is continuously administered for 2 to 3 months (Boorman et al. 1980; Barr et al. 1988). The mechanism behind the cells' ability to resist further injury is not understood.

The original NTP/HEI Collaborative Ozone Project addressed the effects of ozone exposure in F344/N rats at only one examination time point (at the end of a 20-month exposure). Early in the course of our studies, we recognized the deficiencies associated with a single time point. We could not assess the progression of cellular changes throughout the prolonged exposure period, nor adequately interpret changes in antioxidant enzyme levels in the tracheobronchial tree and central acinus. As we analyzed the tissues and interpreted our data from the 20-month exposure, many questions arose that led us to design another study, following the same protocols but for a 3-month duration of exposure, that would provide data to help address these issues. Our primary findings from the 20-month exposure and the issues they raised are briefly described for three areas: the airways, the central acinus, and antioxidant enzymes.

In the airways, the nonciliated cell volume density significantly increased in a dose-dependent manner in the terminal bronchioles of the caudal region of the left lung arising from a long airway path from the trachea. With only one examination point, we could not determine when this hyperplastic remodeling began. In planning the 3-month exposure study, we wanted to examine cells that occupied the same air pathway from the trachea to the distal portion of the acinus, as we had done after the 20-month exposure, and assess the progression of hyperplastic remodeling. Furthermore, we planned to correlate the observed changes with models of ozone dosimetry in the lungs. By following the sampling procedures we used in the 20-month exposure study, we would be able to compare the cellular and antioxidant enzyme changes in site-specific regions of the lungs and evaluate the differences and similarities in ozone dosimetry at the two time points.

In the central acinus, the principal alterations in the ventilatory units after 20 months of exposure were extensions of bronchiolar epithelium (ciliated and nonciliated cells) into the centriacinar alveolar ducts (referred to as bronchiolarization) (Pinkerton et al. 1993) and increases in interstitial volume density. The depth to which bronchiolar epithelium extended beyond the BADJ was concentration-dependent and site-specific. The most prominent changes were noted in male rats in ventilatory units arising from a short airway path (the cranial region), rather than those arising from a long airway path (the caudal region), of the left lung. In the 3-month exposure study, we planned to quantify the degree of epithelial change and the extent and degree of remodeling in the more distal acini using the same sampling procedures and analytic methods we had applied to cells along the bronchial airway tree.

In our studies of antioxidant enzymes after the 20-month exposure, the total SOD activity increased in a concentration-dependent fashion in the distal trachea and terminal bronchioles. We hypothesized that the higher levels of antioxidant enzymes in ozone target sites may be one mechanism by which the cells develop resistance to ozone exposure. To test this hypothesis, we planned to compare the levels of antioxidant enzymes after a shorter exposure with the levels detected after prolonged exposure. Our intent was then to correlate these metabolic alterations, which may in part be responsible for the decreased sensitivity that prolonged ozone exposure produces, with the structural changes in the airways and the central acinus.

Another issue underlying all of the findings from the 20-month exposure is what role the natural aging process of the rat has in the animal's response to ozone. In that exposure protocol, rats were exposed to ozone for nearly their entire life span. Did aging somehow influence their response? Or did the ozone exposure somehow affect the natural aging process? The ozone exposure led to structural changes in the airways, as does the aging process (Pinkerton et al. 1982). What is not known is whether those changes evolved via the same or different mechanisms. Exposing rats to ozone for 3 months and comparing the changes with those found after 20 months would better elucidate which structural changes are due to ozone exposure and which to the aging process.

SPECIFIC AIMS

The overall objective of this study was to define quantitatively the effects of a 3-month exposure to ozone (at 0.0, 0.12, and 1.0 ppm) on target and nontarget sites of the tracheobronchial tree and pulmonary acini, and to compare these data with those from almost identical studies with animals exposed to the same concentrations of ozone for 20 months as part of the NTP/HEI Collaborative Ozone Project. (The exposure protocol and distribution of animal tissues have been described in detail in Project Staff [1995], and the results of our research were presented in Pinkerton et al. 1995.)

This study was designed to address four specific issues:

1. Is the hyperplastic bronchiolar centriacinar remodeling observed after 20 months of ozone exposure present at 3 months of exposure? If so, what is the extent of this remodeling within the pulmonary acinus at 3 months?
2. What is the distribution of the antioxidants Cu-Zn SOD and Mn SOD within the pulmonary acinus at 3 months?
3. Are changes along the respiratory tract that appear to be compensatory after 20 months of exposure due to ozone, or are they aspects of the natural aging process in rats?
4. Is it possible that changes brought about by the natural aging process could override or confound a clear definition of the effects of ozone at ambient concentrations (which are of most public health concern with long-term or prolonged exposure)?

To facilitate comparing 3-month exposure results with those from the 20-month exposure, we followed the exposure protocol designed by the National Toxicology Program, and used the same analytic procedures and techniques we had designed for our earlier studies, with the following exceptions in study design. First, exposure resources at the University of California, Davis (UC Davis) limited the current study to a small group of animals; thus, we could use only two concentrations of ozone (plus a control level of 0 ppm). We used 0.12 ppm ozone (the former National Ambient Air Quality Standard) because it adequately represents an ambient level of human exposure. We chose 1.0 ppm (rather than the other NTP exposure concentration of 0.5 ppm) to provide the greatest contrast with both control and ambient levels.

Second, given the space limitations, we chose to work with only male rats because in the original study, males appeared to have a more marked response to ozone than did females, especially after exposure to 0.12 ppm ozone.

The third exception was our decision not to measure total SOD activity, but to use immunohistochemistry to differentiate between Cu-Zn SOD and Mn SOD. Furthermore, we chose to examine immunohistochemically the distribution of these two forms of SOD after only 2 months of exposure because of the logistical limitations in fixing and processing lungs for different methods of analysis.

METHODS AND STUDY DESIGN

The effects of long-term exposure to ozone in the lower respiratory tract were identified as changes in cell volume density and type, and as alterations in levels of SOD in these same populations of cells. Each level of the respiratory tract was isolated by microdissection techniques to allow for the selection of identical sites for morphometric, histochemical, and enzyme identification studies within target and nontarget regions of the lung.

ANIMAL EXPOSURE PROTOCOL

We designed our exposure protocol to follow exactly that used in the NTP/HEI Collaborative Ozone Project so that data from our 3-month exposure groups could be compared easily with those from the 20-month exposure groups.

Male F344/N rats were obtained from Simonsen Laboratories (Gilroy, CA) at 4 to 5 weeks of age. Each animal was randomly assigned to an ozone exposure or control group after a 10- to 14-day quarantine period. Animals were maintained at the California Regional Primate Research Center at UC Davis, where they were housed in stainless-steel and glass inhalation chambers of 4.2-m^3 capacity. The average temperature range within the exposure chambers over the course of the study was 23.9 to 24.4 °C; the relative humidity range was 57.1% to 60.2%.

Animals were exposed to either ozone or filtered air for a six-hour period each day (between 7:30 a.m. and 5:30 p.m.), five days per week for 3 months. Ozone was generated by corona discharge using an OREC Model 03V5-0 ozonator (Ozone Research and Equipment Corporation, Phoenix, AZ) with 100% oxygen. Ozone concentration in each chamber was monitored by a multiplexed Dasibi Model 1003-AH ultraviolet spectrophometric analyzer (Dasibi Environmental Corporation, Glendale, CA). Calibration of the monitor was accomplished by comparison with a chemical-specific calibrated (neutral-buffered potassium iodide method) monitor simultaneously sampling the exposure chambers. The target concentrations for ozone were 0.00 ppm for the control chamber and 0.12 ppm and 1.00 ppm for the ozone chambers. The actual exposure concentration (mean ± SD) over the course of the study in the

control chamber was less than 0.002 ppm (below the limit of detection), and 0.12 (± 0.01) and 1.01 (± 0.05) ppm in the ozone chambers. To determine concentration uniformity, measurements were periodically made at 12 locations in each chamber. Ambient ozone was removed from all chambers using a potassium permanganate filter. Charcoal and high-efficiency particulate air (HEPA) filters were used to further filter air entering the chambers. Animals were killed one day after the conclusion of the exposure.

The detailed exposure protocol for the 20-month exposure study (the NTP/HEI Collaborative Ozone Project) and the distribution of animal tissues has been reported (Project Staff 1995). Briefly, exposure to ozone was performed at Battelle Pacific Northwest Laboratories (Richland, WA) as part of a collaborative, multilevel study with the NTP and HEI to examine the long-term effects of ozone. Animals were assigned to teams of investigators by a strictly randomized scheme. The animals were free of respiratory disease, as judged by the testing of sentinel animals from each chamber throughout the exposure period and at the end of the study. Animals with leukemia were also identified and examined as a potential confounding factor in morphometric measurements of tissue compartments. At the end of the 20-month exposure, all animals were held for one week before being killed to emphasize permanent, nontransient changes in the lungs.

ANALYSIS OF THE TRACHEOBRONCHIAL TREE AND VENTILATORY UNITS

The analysis of the tracheobronchial epithelium and ventilatory units was based on the assumption that the response of the respiratory tract to ozone is highly heterogeneous and site-specific. We compared the same morphometric parameters for each site examined in the lungs: the trachea; the cranial, central, and caudal bronchi of the left lung lobe; and the proximal and terminal bronchioles arising from these cranial and caudal bronchi. We chose the two parameters of total epithelial volume density and nonciliated cell volume density for rigorous statistical analysis as the most sensitive measures of ozone-induced changes. A minimum of four ventilatory units arising from each airway path followed, i.e., the short-length cranial path and the long-length caudal path, were isolated in longitudinal profile for analysis. The precise cellular localizations of Cu-Zn SOD and Mn SOD were also examined within the parenchymal and centriacinar regions of the lungs for animals exposed to ozone for 2 months.

Lung Fixation and Preparation for Morphometry

Four rats from each of the exposure groups and the control group were randomly selected for evaluation. Animals were killed with an overdose of sodium pentobarbital. The lungs were collapsed by diaphragmatic puncture and fixed in situ by intratracheal instillation of 2% glutaraldehyde in cacodylate buffer (pH 7.4, 350 mOsm) for 15 minutes at 30 cm fixative pressure (Plopper 1990). The fixed lungs were removed by thoracotomy and stored in the same fixative until processing for morphometric analysis. The fixed lungs were trimmed of all mediastinal contents and the lung volumes measured by fluid displacement. Regions of left lung lobe were selected for complementary histochemistry and high-resolution light microscopy.

Tracheobronchial Airway Isolation Beginning with the trachea, airways were dissected along their long axes to approximately the level of the terminal bronchiole (Plopper 1990). The dissections were done with the aid of a Wild M8 dissecting microscope (Wild Heerbrugg Instruments, Farmingdale, NY) and fiber optic illumination. The airway paths selected for study are illustrated in Figure 1 and are identified as the cranial, central, and caudal regions. As summarized

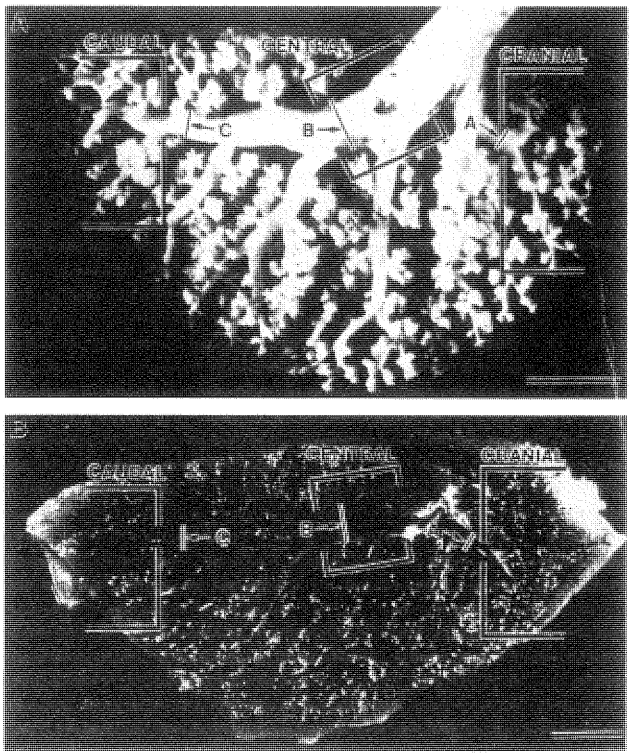

Figure 1. Location of tissue samples taken from the rat lung. (A) Silicone cast of the tracheobronchial airway tree. Lung casts served to standardize sampling. Samples of terminal BADJs were taken from the three regions (cranial, central, and caudal) indicated with letters and arrows within the figure. (B) Mediastinal half of a fixed, microdissected rat lung. Note how closely the pathways and sampling regions match the silicone cast shown above. Bar = 4 μm.

in Table 1, the cranial region included a medium-sized conducting airway with a short path length, a large cumulative angle of change in the path direction, and a relatively small diameter. The cranial centriacinar regions were selected from the acini supplied by this bronchial pathway. The conducting airway selected from the central region had the same number of generations of branching as that of the cranial region, but was much larger in diameter and was part of the axial pathway for conducting airways in the left lobe. The airway selected from the caudal region had a much greater path length and approximately the same diameter as that of the cranial bronchus; however, the angle of deviation was much less in the caudal airway. The caudal centriacinar regions were selected from the acini supplied by this airway.

Identifying airway location during dissection was facilitated by using silicone casts prepared from the lungs of three 4- to 5-month-old male F344/N rats. Each cast was prepared according to a modified saline displacement casting procedure in which silicone rubber (Dow Corning Silastic 734 RTV, Dow Corning Corporation, Midland, MI) was injected into the trachea at 25 mPa (cm H_2O) positive pressure. After curing for two days, the silicone-filled lungs were surgically removed from the thorax and boiled in 1 N sodium hydroxide to remove the lung tissue. Casts were trimmed to reveal airways from the major bronchus to the level of the terminal bronchioles. The path length and cumulative branch angle of each airway were measured directly from the casts.

The rat lung has a monopodial form of airway branching in which both a major and a minor daughter airway arise from each parent airway. A labeling system devised by Phalen and associates (Phalen et al. 1978; Phalen and Oldham 1983) exploits this unique arrangement and uses a binary numbering scheme to label all sequential major airways as "1" and all minor airways as "0." Beginning at the trachea (designated as 1), the classification of each new airway generation is added to give a unique branching history for each pathway. These branching histories were easily and reliably determined from the lung casts and were used as guides to ensure that dissections in the fixed, wet lungs followed identical pathways to each region in every lung. Table 1 summarizes the branching history, generation number, path length, diameter, and cumulative branch angle for each airway followed. The most distal airways revealed by microdissection were usually two to four generations from the terminal bronchioles. Blocks of tissue approximately 1.5 × 1.5 × 0.4 μm in size were cut in a plane perpendicular to the axis of the most distal dissected airway to isolate parenchymal tissue arising from each dissected pathway.

For the cranial, central, and caudal regions, blocks were removed and embedded as large blocks in glycolmethacrylate. Sections 1.5 μm thick were cut with glass knives on a JB4 microtome. Serial and serial-step sections were stained with Alcian blue/periodic acid–Schiff (pH 2.5) or toluidine blue (0.5% in 1% borate) to facilitate the identification of nonciliated cells containing intracellular secretory product.

Ventilatory Unit Isolation The areas selected for study were from the cranial and caudal regions of the lung at the distal ends of two conducting airway paths, one in which air travels a short path length with a large cumulative angle of change in the path direction and the other selected from a region served by a much greater path length and low angle of deviation (Table 1). These regions in the left lung are identified as cranial and caudal sites respectively (Figure

Table 1. Characteristics of Airway Samples

Airway	Generation Number	Path Length (mm)	Cumulative Branch Angle (°)	Diameter (mm)
Distal trachea	0	NA[a]	NA	3.3 ± 0.1
Lobar bronchus	1	6.7 ± 0.1	15 ± 0.0	2.8 ± 0.1
Cranial region bronchus	4-5	11.7 ± 0.9	140 ± 15	0.7 ± 0.0
Cranial region central acinus	8-10	14.0 ± 1.2	225 ± 21.8	—
Central region bronchus	4-5	11.2 ± 0.3	8.3 ± 5.8	2.4 ± 0.1
Central region central acinus	6-7	13.7 ± 1.1	50 ± 8.7	—
Caudal region bronchus	10-12	20.2 ± 0.4	30.0 ± 8.6	1.0 ± 0.1
Caudal region central acinus	15-16	22.3 ± 0.3	30.0 ± 8.6	—

[a] NA = not applicable.

1). The tissue blocks selected by microdissection were usually two to four generations from the terminal bronchioles. After dissection, blocks were removed and embedded as large blocks in Araldite 502. Tissue slices (approximately 2 × 4 × 6 μm in size) were post-fixed in 1% osmium tetroxide in Zetterquist's buffer, followed sequentially by 1% tannic acid and 1% uranyl acetate in maleate buffer, dehydrated in ethanol and propylene oxide, and embedded in either Epon 812 or Araldite 502.

Systematically measuring the distribution of tissue changes in ventilatory units of animals exposed to ozone requires a strategy that insures the proper identification of the BADJ. If these junctions are not identified correctly, inappropriate comparisons of mismatched alveolar duct generations may occur between control and treated animals. After exposure to high concentrations of ozone, the bronchiolar epithelium can extend from the level of the terminal bronchiole into the proximal alveolar regions of the ventilatory unit (Boorman et al. 1980; Barr et al. 1988). Such a change potentiates the possibility of inadvertent comparisons of first alveolar duct generations in control animals to second- and third-order generations of alveolar ducts in the lungs of animals exposed to ozone. However, if no alveoli are obliterated during the process of epithelial reorganization, the first alveolar outpocketing along the airway path may serve as a landmark for the identification of the original BADJ.

From each embedded tissue block, BADJs were isolated by the methods of Pinkerton and associates (1993). Centriacinar regions were isolated by cutting the entire tissue block into slices approximately 0.4 to 0.5 μm thick. Each slice was examined under a dissecting microscope to identify BADJs in longitudinal profile (Figure 2). The criterion for selection was a symmetrical pair of alveolar ducts arising from a single terminal bronchiole. Isolations meeting this selection criterion consistently contained alveolar duct paths in longitudinal profile that extended two to four generations beyond the BADJ. Selected isolations were remounted on BEEM capsules and sectioned at a thickness of 0.5 μm with glass knives. Sections were stained with toluidine blue (0.5% in 1% borate buffer).

Morphometry

Tracheobronchial Airways The volume density of conducting airway epithelial cells were evaluated by procedures that have been discussed in detail elsewhere (Hyde et al. 1990; Hyde et al. 1992; Plopper et al. 1992). All measurements were made with high-resolution light microscopy (×40 objective and 0.5- to 1.0-μm sections) from video images captured with a DAGE MTI video camera (Michigan City, IN) mounted on an Olympus BH-2 microscope, which was interfaced with a Macintosh IIci computer running NIH IMAGE software. The analysis was performed by means of a cycloid grid overlay and software for counting points and

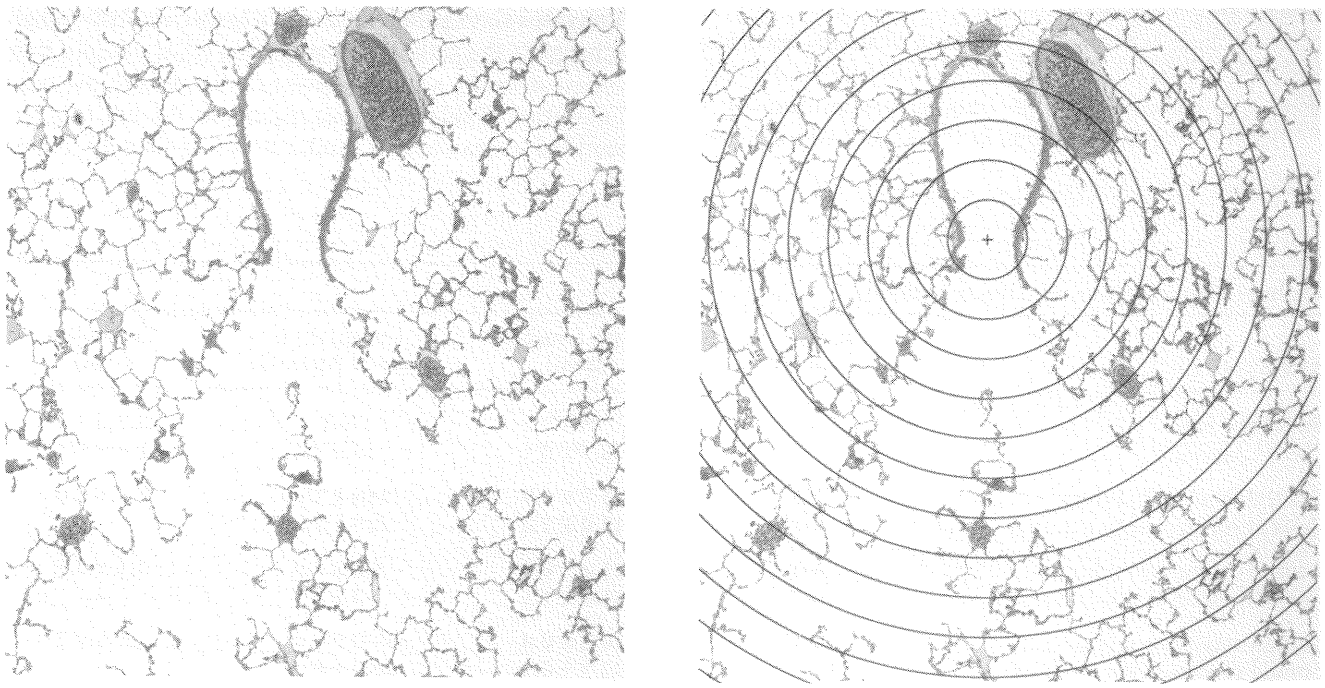

Figure 2. Ventilatory unit isolation (left), with a concentric overlay to define 100-μm intervals (right).

intercepts (Stereology Toolbox, Davis, CA) (see Hyde et al. 1990, 1992 for detailed description of grids and counting procedures). The volume densities (V_v) of three categories of cells (nonciliated, ciliated, and basal) were determined by point counting and were calculated with the formula:

$$V_v = P_p = P_n/P_t$$

where P_p is the point fraction of P_n, the number of test points hitting the structure of interest, divided by P_t, the total points hitting the reference space (epithelium). The surface area of epithelial basement membrane per reference volume (S_v) was determined by point and intercept counting and was calculated with the formula:

$$S_v = 2\ I_O/L_r$$

where I_O is the number of intercepts with the object (epithelial basal lamina) and L_r is the total length of test line in the reference volume (epithelium). To determine the total epithelial volume density (which is the sum of the volume densities of nonciliated, ciliated, and basal cell categories), the epithelial volume per unit of basal lamina surface area ($\mu m^3/\mu m^2$) was calculated with the formula for arithmetic mean thickness (t) of the epithelium:

$$t = V_v/S_v$$

For each bronchus and the trachea, four fields were evaluated. Fields were randomly selected by dividing the cross section of the airway into four quadrants, choosing a random angle (between 0° and 90°) from a random number table and centering the field for evaluation on that angle. In the centriacinar region, at least five areas were analyzed. Epithelium identified as the terminal bronchiole was defined as the epithelium just proximal to the first alveolar outpocketing. Epithelium defined as proximal bronchiole was obtained from a site contiguous with the terminal bronchiole, but 0.5 to 1 μm more proximal than that area.

Ventilatory Units Each ventilatory unit isolation was captured as a digital video image on the computer. From a single reference point at the level of the first alveolar outpocketing, a pattern of concentric arcs at 100-μm intervals was placed over the isolation (Figure 2). These digital images for each isolation served as guides to identify arc intercepts with tissues along the ducts of each ventilatory unit. Only those regions within the concentric circles that overlay tissues along open duct paths within a 30° angle incident to either side of a line bisecting the ventilatory unit profile were measured.

Alveolar septal tips within each 100-μm interval were selected by random number generation and analyzed. Images captured at ×400 were used for epithelial, interstitial, and capillary lumen volume density measurements with a test lattice overlay (21 lines) to perform point and intercept counts to derive volume and surface densities. All volume measurements were normalized to the alveolar surface. In this study, surface area was defined as the alveolar tissue-air interface. A total of four to eight isolations per animal were analyzed. These measurements were made at each 100-μm interval down the alveolar duct path. Data from the total number of measurements per 100-μm interval were averaged and expressed as epithelial, interstitial, and capillary lumen volume density. Tissue density was derived by point and intercept counts from each field analyzed. All counts were compiled and imported into a spreadsheet, then the data were organized and calculations performed to determine volume densities for the epithelium, interstitium, and capillary lumen. In addition, alveolar macrophages, although not part of the septal wall, were measured as a volume density normalized to the alveolar surface within each 100-μm interval in which these cells were found.

ANTIOXIDANT ENZYME LOCALIZATION

Antibodies

The antisera to Cu-Zn SOD is a rabbit anti-rat Cu-Zn SOD polyclonal sera and has been described previously (Slot et al. 1986). The antibody is specific for Cu-Zn SOD and the reaction can be absorbed by purified Cu-Zn SOD (Chang et al. 1988a). The antisera to Mn SOD is a rabbit anti-human Mn SOD sera made with recombinant human Mn SOD (Boehringer Ingelheim Pharmaceuticals, Inc., Ridgefield, CT). The antisera is monospecific for a single protein at a molecular weight corresponding to Mn SOD on immunoblots. Coincubation of the antisera with antigen abolishes the reaction on immunoblots (Kinnula et al. 1994). This polyclonal antisera cross-reacts with rat Mn SOD.

Lung Fixation and Preparation for Light Microscopy (Immunohistochemistry)

Within 24 hours of the end of 3 months of ozone exposure, animals were anesthetized and then killed with sodium pentobarbital, and each trachea was cannulated. Both hemidiaphragms were punctured to deflate the lungs. The lungs were fixed by instillation of neutral buffered formalin at 20 cm H_2O and stored in 70% ethanol for 24 hours before embedding in paraffin. The blocks were sectioned at 5 μm and labeled with Mn SOD (1:1,000) or Cu-Zn SOD (1:10,000 or 1:100,000) using the avidin biotin peroxidase method with reagents from Vector Laboratories (Burlingame, CA), visualized with 3,3′-diaminobenzidine tetrahydrochloride from Sigma (St. Louis, MO) and counterstained with May-

ers hematoxylin (Sigma). The two different concentrations of Cu-Zn SOD were used to determine the relative abundance of Cu-Zn SOD in specific regions of the lung. Photomicrographs were made on a Zeiss Axioskop MC80 with Fuji Reala color film.

Lung Fixation and Preparation for Electron Microscopy (Immunogold Labeling)

The lungs of animals exposed to ozone for 2 months were fixed by instillation of 0.25% glutaraldehyde in 0.1 M sodium cacodylate (pH 7.4) at 20 cm H_2O. After fixation for 10 minutes in the chest, the accessory lobe of the lungs was removed and stored in 0.25% glutaraldehyde until processed.

Slabs of tissue taken from the lung were washed in 1.5 M phosphate-buffered saline (PBS) plus 0.2 M glycine, infiltrated for 10 minutes with 2% gelatin in 1.5 M PBS, followed by 5% gelatin in 1.5 M PBS for 10 minutes, and finally 10% gelatin in 1.5 M PBS for 10 minutes. Following the last change in gelatin, the tissue was transferred onto a glass slide on ice and allowed to harden. Tissue slices were examined under a dissecting microscope in a cold room, and terminal bronchioles were identified in longitudinal orientation using a modification of the method of Barry and associates (1985). Areas containing a terminal bronchiole and proximal alveolar ducts in longitudinal orientation were cut out as a cube and then infiltrated with 2.3 M sucrose overnight at 5°C using a rotator. The tissue blocks were then frozen in liquid nitrogen, dehydrated in methanol at −90°C and embedded in Lowicryl resin at −45°C following the method of Oprins and associates (1994). The longitudinally oriented blocks were polymerized with UV light and sectioned on an LKB ultramicrotome. This method maintained the antigenicity of the enzyme and allowed longitudinally oriented sections to be cut. Ultrathin sections were mounted on formvar and carbon-coated copper grids.

Sections were labeled following the methods of Slot and Geuze (1984, 1985). Briefly, the tissue sections were washed in 1.5 M PBS + 0.1% bovine serum albumin (BSA), labeled with diluted (1:300) Mn SOD antisera for 60 minutes, washed several times in PBS + 0.1% BSA and placed on drops of 10-nm protein A-gold. They were then washed in PBS, fixed with 1% glutaraldehyde for 5 minutes, and subsequently washed with multiple changes of distilled water for a total of 1 hour.

Tissue sections from a single block were mounted on glass slides and photographed at low magnification for purposes of orientation. The labeled thin sections were viewed with a Zeiss 10-C electron microscope at ×20,000 by means of a camera system in which a point-counting overlay of 42 points was placed directly on the screen and all cell counts were taken directly from the screen. Each point on the screen covered an area of 0.21 μm^2. All alveolar ducts were examined and type II epithelial cells found in the alveolar duct region were counted as a function of distance from the BADJ. Ten type II epithelial cells were selected randomly at each site in the alveolar ducts. This sampling method included the majority of type II cells present in most sites. Type II epithelial cells were selected from alveolar ridges and outpocketings that directly opened on the alveolar duct. Adjacent closed alveolar profiles were not sampled because it would have been difficult to determine the distance of these alveoli from the BADJ. The type II epithelial cells were sampled as a function of distance from the terminal bronchiole by cells being taken at 200-μm intervals. Specimens from the 0- to 200-μm and 200- to 400-μm intervals were pooled due to a reduced sample size in the 0- to 200-μm interval because the alveolar epithelium had become bronchiolarized from ozone exposure. In addition, type II cells found in the more distal lung parenchyma were sampled by isolating alveolar ducts located farther than 600 μm from the BADJ and counting 10 cells randomly selected per site.

Since Mn SOD is predominantly within the mitochondria, the quantitative analysis of Mn SOD by electron microscope was done examining only mitochondria. The first mitochondrial profile encountered in each cell was selected for counting and points on the mitochondria and the number of gold grains on the mitochondria were tallied. The degree of background labeling was calculated as the relative density of gold grains found on air spaces and this background was subtracted from the relative density of gold grains on mitochondria to give the specific labeling for Mn SOD. Clara cells in terminal bronchioles were counted using a similar method. Clara cells were randomly selected by choosing every other cell from each of the two sides of the longitudinal section through a terminal bronchiole for a total of 10 cells. Immunogold labeling over these cells was counted using the camera system at ×20,000, and total Mn SOD was calculated in the same manner as the type II cells. Fibroblasts were counted by photographing 10 randomly selected cells per site and printing them at ×41,000. These electron micrographs were placed under a point-counting overlay and the point density per cell and gold grain density per cell were determined. Each point on the overlay covered an area of 0.21 μm^2. Fibroblasts in the alveolar ducts were selected by moving radially outward from the BADJ to a distance of 400 μm and counting every fibroblast encountered until 10 cells were selected. All data were calculated as the number of gold grains per points on mitochondria.

Following the methods described above, cells in the bronchiole-alveolar duct region were labeled for Cu-Zn SOD and qualitatively examined. The density of Cu-Zn SOD labeling over type I epithelial cells lining alveolar septa in the proximal alveolar region had been quantified in a preliminary experiment, which showed no detectable difference between the controls and the experimental sites. Because no significant increase of Cu-Zn SOD to ozone exposure in the proximal alveolar region was indicated by either light or electron microscopic immunohistochemistry, we decided that further examination of the Cu-Zn SOD enzyme in this location should be discontinued in favor of assessing changes in the Mn SOD enzyme.

STATISTICAL METHODS AND DATA ANALYSIS

TRACHEOBRONCHIAL AIRWAYS

Volume densities were calculated for ciliated, nonciliated, and basal cells at defined locations in the trachea, and on large bronchi located cranially, centrally, and caudally in the left lobes of the lungs of rats exposed to ozone for 3 months and compared with those exposed earlier for 20 months. The ozone exposure concentrations were 0.12 ppm or 1.0 ppm in addition to an air control group. Volume densities were also calculated for the same cell types in a proximal and a terminal bronchiole located distal to the cranial and the caudal bronchi. The measurements made on the centriacinar bronchioles were analyzed separately from those made on the trachea and large bronchi.

Following the methods described earlier (Pinkerton et al. 1995), the measured variables were identified as either primary or confirmatory. The statistical analyses were performed separately for each variable. Of the three primary variables analyzed after the 20-month exposure, only two were analyzed in the present study: nonciliated cell volume density and total epithelial volume density. The confirmatory variables were ciliated cell and basal cell volume densities, as in the 20-month study.

The complete statistical analysis consisted of up to three steps. The same procedure was followed for each variable, whether it was primary or confirmatory.

First, a multivariate vector of the dependent variables was analyzed with a multivariate analysis of variance (MANOVA). The independent variables were ozone exposure concentration, duration of exposure (time), and the interaction between these two factors. The multivariate vector consisted of the measurements of a single primary or confirmatory variable made at the four large airway sites (trachea, cranial bronchus, central bronchus, caudal bronchus) for the bronchial data. The multivariate vector was analyzed with a two-way repeated measures formulation for the four sites (cranial proximal bronchiole, cranial terminal bronchiole, caudal proximal bronchiole, caudal terminal bronchiole) for the centriacinar data. The two repeated measures factors were site (cranial or caudal) and airway (proximal or terminal). Statistical significance ($p < 0.05$) for the multivariate stage of the analysis was tested with the Hotelling-Lawley trace. If none of the effects were statistically significant in the multivariate analysis, no further statistical testing was performed.

If significant multivariate effects were found, the second stage of the analysis proceeded: analyses of variance (ANOVA) were individually performed for each of the dependent variables of the multivariate vector. For the variables analyzed with two-way repeated measures, it was possible to test for effects of the two multivariate factors (site and airway) and their interaction. If either the interaction or both factors were significant, then the second stage of the analysis was implemented for each dependent variable, as described above. However, if only one of the multivariate factors was significant, the data were averaged before implementing the ANOVA. For example, if a significant effect was found for site but not for airway, the data for measured responses in the proximal and terminal bronchioles at each site (cranial or caudal) were averaged before performing the ANOVA. Statistical significance ($p < 0.05$) for the factors of the ANOVAs was assessed with F tests.

In the third step of the analysis, the levels of the statistically significant factors were subtested with t tests. These t tests were not corrected for multiple comparisons due to the step-down nature of the statistical analysis.

VENTILATORY UNITS

Volume density measurements were made of the epithelium, interstituim, macrophages, and capillary lumen at 100-μm intervals from the beginning of the alveolar duct out to 800 μm. The pattern of epithelial volume density response to ozone exposure is not linear as a function of distance into the ventilatory unit. This response contrasts with the pattern of the volume density response in the interstitium and for macrophages and capillary lumen, which is relatively constant as a function of distance into the ventilatory unit (Pinkerton et al. 1995). As a result, the statistical analysis of the epithelial data differs from the analyses of the other endpoints.

As illustrated by the results of the 20-month study, epithelial volume density is relatively thick near the entrance of the ventilatory unit, but rapidly thins. For example, epithelial volume density in the control animals at the end of the 20-month exposure was approximately 3 to 4

$\mu m^3/\mu m^2$ at 100 μm into the ventilatory unit, but dropped rapidly to a value of approximately 0.2 to 0.3 $\mu m^3/\mu m^2$, which was observed at all distances beyond about 300 μm (Pinkerton et al. 1995). In animals exposed to various concentrations of ozone for 20 months, the epithelial volume density observed near the entrance of the ventilatory unit remained consistent without decreasing for some distance into the ventilatory unit. It then followed a pattern similar to that in the control rats, but offset as a function of distance (Pinkerton et al. 1995). Based on these patterns of response, the analysis strategy summarized here was developed (Pinkerton et al. 1995).

Briefly, a nonlinear regression of two or three linear segments was fit to the volume density measurements at each site (cranial and caudal) for each animal. A schematic of the curve with the parameters estimated is shown in Figure 3. Of interest for this study was the epithelial volume density estimated at or near the entrance of the ventilatory unit (A0, estimated at 100 μm); the epithelial volume density in the distal portion of the ventilatory unit (A3, estimated at X2 μm); and the distance into the ventilatory unit that the volume density is constant (X1 μm); and the estimate of the rate at which the volume density decreased from its initial plateau to its distal plateau (B2). Also included in the statistical analysis was the estimate of variability in the curve fit, the sum of squares due to error (SSE).

The advantage of this model is that the parameters have biologically meaningful interpretations and may be used to test the following hypotheses:

1. Is there a difference associated with ozone exposure in the initial value of epithelial volume density (A0)?
2. Is there a difference associated with ozone exposure in the distal value of epithelial volume density (A3)?
3. Is there a difference associated with ozone exposure in the distance into the ventilatory unit that the epithelial volume density remains elevated at its initial value (X1)?

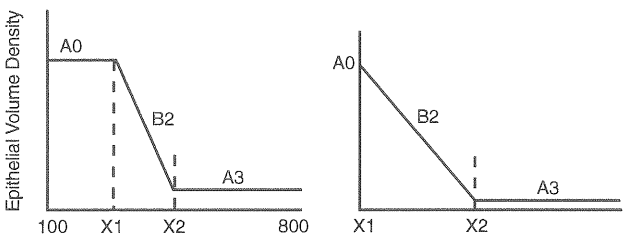

Figure 3. Linear regression model fit to epithelial volume density parameters of the ventilatory unit of the lung. Five parameters were fit to describe the epithelial volume density for three (left panel) or two (right panel) linear segments. For some rats (left), an initial plateau in thickness (A0) was observed from 100 μm to point X1 down the alveolar duct path of the ventilatory unit. For rats without this plateau (right), parameter A0 is the *y* intercept for the linearly declining segment, and X1 = 100 μm. After a linearly declining segment described by its slope (B2), a lower flat segment was observed (A3), which began at X2 μm distal from the terminal bronchiole and continued through 800 μm.

4. Is there a difference associated with ozone exposure in the distance into the ventilatory unit at which the epithelial volume density descends to its lower value (X2)?
5. Is there a difference in how rapidly the epithelial volume density decreases as a function of distance (B2)?

The five estimated parameters (A0, A3, X1, X2, B2) and the SSE were analyzed in two or three MANOVAs: first, for the difference between the cranial and caudal sites; and then as the average of the cranial and caudal sites if no statistically significant differences were detected between the sites, or separately for the two sites if the first MANOVA indicated that there were statistically significant differences between the sites. Multivariate significance was identified as $p < 0.05$ using the Hotelling-Lawley trace. The independent variables in these analyses were ozone exposure concentration, duration of exposure (time), and the interaction between these two factors. If a statistically significant MANOVA effect was found, the univariate ANOVAs were examined for statistically significant effects of the independent variables for each parameter. Finally, significant ANOVA effects were tested using uncorrected *t* tests generated from the least squares means. Because of the multiple levels of testing, no multiple comparison correction factors were applied to the *t* tests.

The other endpoints (capillary lumen, macrophage, and interstitial volume densities) were analyzed with a repeated measures multivariate analysis. The vector of dependent variables consisted of the three volume densities in each of the eight 100-μm intervals (0 to 100 μm, 100 to 200 μm, etc.) in the ventilatory unit for each of the endpoints. As described for the epithelial volume density, the data were first analyzed as the difference between the cranial and caudal sites. If statistically significant multivariate effects were found, the two sites were analyzed separately; otherwise, the data for each animal were averaged and analyzed without separate consideration of site. If significant effects were found in the repeated measures analyses, the individual ANOVAs for each distance interval were examined for statistically significant relationships due to ozone exposure concentration, length of exposure, and the interaction of these two factors. Significant ANOVA effects were subtested with *t* tests of the least squares means. Before performing the multivariate analyses, the data vectors were tested for homogeneity of variance and normalized as appropriate.

ANTIOXIDANT ENZYME LOCALIZATION

Statistical analysis was applied only to the immunogold staining for Mn SOD localization in the lungs as seen by electron microscopy. As has been described earlier in the

methods for immunogolding labeling, the number of gold grains per points on mitochondria were expressed as means ± SEM. Student's *t* test was used to determine statistical relevance.

RESULTS

TRACHEOBRONCHIAL AIRWAYS

For the evaluation of changes in the epithelial components of the conducting airways (Tables 2 and 4), the data for the trachea, central, cranial, and caudal intrapulmonary airways were considered as a set and comparisons made based on site, exposure concentration, and duration of exposure (Tables 3 and 5).

When changes in ciliated cell volume density in the large airways (Table 2) were compared by MANOVA, a significant effect was associated with ozone concentration (Table 3). This effect was observed only in the caudal region. Because it is a main factor effect, the mean (± SEM) ciliated cell volume density for each ozone concentration was averaged over 3 and 20 months of exposure and is listed here:

Table 2. Volume Density of Epithelial Cells of Rat Tracheobronchial Airways After Exposure to Ozone for 3 or 20 Months[a]

Ozone Concentration (ppm)	Length of Exposure (months)	Airway and Region			
		Trachea	Bronchus		
		Distal	Cranial	Central	Caudal
Ciliated Cells					
0.0	3	2.81 ± 0.26	4.50 ± 0.88	2.74 ± 0.33	4.73 ± 0.33
0.12		2.12 ± 0.18	4.78 ± 0.43	3.36 ± 0.79	3.97 ± 0.33
1.0		3.03 ± 0.41	4.24 ± 0.31	2.96 ± 0.28	3.99 ± 0.30
0.0	20	4.25 ± 0.84	3.80 ± 0.56	3.33 ± 0.29	5.17 ± 0.73
0.12		3.26 ± 1.21	4.83 ± 0.81	4.20 ± 0.73	6.25 ± 0.61
1.0		2.32 ± 0.39	3.95 ± 0.25	2.56 ± 0.68	2.89 ± 0.76
Noncilitated Cells					
0.0	3	1.87 ± 0.29	1.73 ± 0.30	2.07 ± 0.28	1.83 ± 0.40
0.12		2.50 ± 0.08	1.77 ± 0.27	1.87 ± 0.38	1.69 ± 0.24
1.0		2.39 ± 0.49	1.42 ± 0.18	1.84 ± 0.30	1.06 ± 0.14
0.0	20	3.15 ± 0.53	2.20 ± 0.52	1.89 ± 0.22	2.65 ± 0.45
0.12		4.28 ± 0.56	1.71 ± 0.46	2.18 ± 0.49	2.17 ± 0.38
1.0		3.22 ± 0.30	2.92 ± 0.66	2.53 ± 0.36	2.10 ± 0.26
Basal Cells					
0.0	3	0.17 ± 0.13	0.00 ± 0.00	0.08 ± 0.03	0.02 ± 0.02
0.12		0.18 ± 0.04	0.02 ± 0.02	0.05 ± 0.04	0.02 ± 0.02
1.0		0.27 ± 0.14	0.00 ± 0.00	0.10 ± 0.05	0.00 ± 0.00
0.0	20	0.20 ± 0.13	0.00 ± 0.00	0.09 ± 0.06	0.00 ± 0.00
0.12		0.16 ± 0.12	0.00 ± 0.00	0.05 ± 0.03	0.00 ± 000
1.0		0.19 ± 0.11	0.00 ± 0.00	0.12 ± 0.05	0.09 ± 0.06
Total Epithelial Volume Density					
0.0	3	4.84 ± 0.59	6.23 ± 0.67	4.89 ± 0.43	6.58 ± 0.31
0.12		4.80 ± 0.19	6.57 ± 0.62	5.28 ± 0.62	5.67 ± 0.44
1.0		5.69 ± 0.59	5.66 ± 0.42	4.90 ± 0.41	5.05 ± 0.31
0.0	20	7.60 ± 0.83	6.01 ± 0.66	5.30 ± 0.55	7.82 ± 1.16
0.12		7.70 ± 1.36	6.54 ± 0.83	6.43 ± 0.87	8.42 ± 0.98
1.0		5.73 ± 0.72	6.87 ± 0.50	5.21 ± 0.66	5.08 ± 0.95

[a] Values are presented as means ± SEM expressed as $\mu m^3/\mu m^2$; $n = 4$ for each ozone concentration group.

Ciliated cell volume density in the caudal region after exposure to 0.0 ppm ozone was 4.95 ± 0.36; after 0.12 ppm ozone it was 5.11 ± 0.34; and after 1.0 ppm ozone it was 3.44 ± 0.36. There was no statistically significant difference in ciliated cell volume density following exposure to 0.12 ppm ozone when compared with control. There was, however, a significant decrease in ciliated cell volume density at the caudal site following exposure to 1.0 ppm ozone.

For nonciliated cell volume density (Table 2), based on MANOVA, a significant time effect was found (Table 3). By ANOVA, significant time effects were observed in the trachea and caudal region. Because there were only two groups (3 or 20 months), no further subtesting was required. The means (± SEM) for nonciliated cell volume density in the trachea were 2.25 ± 0.21 at 3 months and 3.55 ± 0.24 at 20 months. The means at the caudal site were 1.53 ± 0.17 and 2.31 ± 0.20, at 3 and 30 months, respectively.

Table 3. Statistical Significance[a] of Parameters Describing Epithelial Cell Characteristics of the Trachea and Bronchi

Variable and Site	Statistical Analysis[b]	Time	Concentration	Concentration × Time
Primary Variables				
Total epithelial volume density	Multivariate	0.08	0.15	0.38
Trachea	Univariate			
Cranial				
Central				
Caudal				
Nonciliated cell volume density	Multivariate	< 0.01*	0.20	0.52
Trachea	Univariate	< 0.01*		
Cranial		0.06		
Central		0.36		
Caudal		0.01*		
Confirmatory Variables				
Ciliated cell volume density	Multivariate	0.52	0.01*	0.11
Trachea	Univariate		0.27	
Cranial			0.42	
Central			0.22	
Caudal			0.01*	
Basal cell volume density	Multivariate	0.79	0.68	0.26
Trachea	Univariate			
Cranial				
Central				
Caudal				

[a] An asterisk (*) indicates a significant effect ($p < 0.05$) that determined the next level of analysis.

[b] As described in the Methods section, a step-down analysis procedure was used. In the first step, a MANOVA was performed for the vector of responses for a single variable at the four sites. (The results of this analysis are reported in the row showing "multivariate" in the second column.) If the MANOVA detected significant effects, we continued with the next level of analysis for that variable and conducted an ANOVA for each of the sites. If no significant effect was found using the MANOVA, the next level of analysis was not done and that block of the table is empty. The independent variables were the same for MANOVAs and ANOVAs.

For total epithelial volume density (Table 2), there were no significant effects found at the multivariate level (Table 3).

In terminal and proximal bronchioles, ciliated cell volume density (Table 4) demonstrated a four-way interaction, so the individual ANOVAs are reported (Table 5). Despite the overall interaction, there were no significant effects in the individual ANOVAs.

For nonciliated cells in terminal and proximal bronchioles (Table 5) there was a statistically significant multivariate interaction between the sites and ozone concentration so the average value of the proximal and terminal bronchioles at each site was calculated and those values analyzed in an ANOVA identified as a 'Site ANOVA' in Table 5. In the cranial site there was a statistically significant differ-

Table 4. Volume Density of Epithelial Cells of Rat Proximal and Terminal Airways in Cranial and Caudal Regions of the Lung After Exposure to Ozone for 3 or 20 Months[a]

Ozone Concentration (ppm)	Length of Exposure (months)	Airway and Region			
		Proximal		Terminal	
		Cranial	Caudal	Cranial	Caudal
Ciliated Cells					
0.0	3	6.13 ± 0.89	5.68 ± 0.60	4.54 ± 0.27	4.44 ± 1.52
0.12		6.59 ± 1.43	4.94 ± 1.11	4.20 ± 0.08	3.74 ± 0.09
1.0		3.85 ± 1.09	4.74 ± 0.13	5.66 ± 1.60	3.26 ± 0.46
0.0	20	4.67 ± 0.22	5.16 ± 0.29	4.37 ± 0.75	4.29 ± 0.49
0.12		4.88 ± 0.42	3.95 ± 0.39	3.90 ± 0.09	4.28 ± 0.23
1.0		4.33 ± 0.86	3.83 ± 0.61	2.62 ± 0.41	2.77 ± 0.25
Nonciliated Cells					
0.0	3	3.44 ± 0.36	2.99 ± 0.75	4.10 ± 1.07	3.72 ± 0.36
0.12		3.25 ± 0.22	2.58 ± 0.27	2.44 ± 0.31	2.45 ± 0.94
1.0		3.82 ± 1.10	4.22 ± 0.83	3.09 ± 0.95	4.19 ± 0.67
0.0	20	3.04 ± 0.25	2.69 ± 0.85	2.66 ± 0.26	2.38 ± 0.29
0.12		2.20 ± 0.20	2.44 ± 0.31	2.40 ± 0.17	3.44 ± 0.42
1.0		2.10 ± 0.07	3.22 ± 0.30	3.07 ± 0.31	4.21 ± 0.32
Total Epithelial Volume Density					
0.0	3	9.57 ± 0.66	8.67 ± 0.61	8.64 ± 1.31	8.16 ± 1.16
0.12		9.84 ± 1.65	7.53 ± 1.38	6.64 ± 0.38	6.19 ± 1.02
1.0		7.67 ± 1.34	8.96 ± 0.70	8.74 ± 0.78	7.45 ± 0.34
0.0	20	7.71 ± 0.23	7.85 ± 0.90	7.03 ± 0.72	6.67 ± 0.31
0.12		7.08 ± 0.25	6.39 ± 0.38	6.30 ± 0.16	7.72 ± 0.56
1.0		6.42 ± 0.89	7.05 ± 0.53	5.69 ± 0.37	6.98 ± 0.32

[a] Values are presented as means ± SEM expressed as $\mu m^3/\mu m^2$; $n = 4$ for each ozone concentration group.

Table 5. Statistical Analysis[a] of Proximal Bronchiole–Terminal Bronchiole Data of Rats Exposed to Ozone

Analysis[b] and Factor[c]	Primary Variables		Confirmatory Variable
	Nonciliated Cell Volume Density	Total Epithelial Volume Density	Ciliated Cell Volume Density
Repeated Measures			
Site	0.25	0.65	0.27
Site × time	0.25	0.09	0.38
Site × concentration	0.05*	0.36	0.75
Site × concentration × time	0.70	0.74	0.98
Airway	0.47	0.04*	0.01
Airway × time	0.35	0.27	0.67
Airway × concentration	0.93	0.66	0.78
Airway × concentration × time	0.11	0.18	0.11
Site × airway	0.33	0.55	0.87
Site × airway × time	0.81	0.43	0.17
Site × airway × concentration	0.79	0.11	0.04
Site × airway × concentration × time	0.90	0.25	0.03*
Time	0.05*	< 0.01	0.03
Concentration	0.05	0.10	0.03
Concentration × time	0.42	0.43	0.81
Individual ANOVAs			
Cranial proximal bronchiole			
Time			0.19
Concentration			0.12
Concentration × time			0.34
Cranial terminal bronchiole			
Time			0.08
Concentration			0.85
Concentration × time			0.12
Caudal proximal bronchiole			
Time			0.08
Concentration			0.09
Concentration × time			0.89
Caudal terminal bronchiole			
Time			0.95
Concentration			0.13
Concentration × time			0.75
Airway ANOVAs			
Proximal			
Time		< 0.01*	
Concentration		0.21	
Concentration × time		0.86	
Terminal			
Time		0.06	
Concentration		0.27	
Concentration × time		0.09	
Site ANOVAs			
Cranial			
Time	0.03*		
Concentration	0.23		
Concentration × time	0.89		
Caudal			
Time	0.36		
Concentration	0.01*		
Concentration × time	0.30		

[a] An asterisk (*) indicates a significant effect ($p < 0.05$) that determined the next level of analysis.

[b] As described in the Methods section, a step-down analysis procedure was used. In the first step, a two-way repeated measures analysis was performed. Depending on the statistically significant effects, we conducted individual ANOVAs or ANOVAs for which dependent variable data were averaged (see the Methods section for details). If no significant effect was found, the next level of analysis was not done and that block of the table is empty.

[c] Factors include site (cranial or caudal), airway (proximal or terminal), time (3 or 20 months), and concentration (0.0, 0.12, or 1.0 ppm ozone).

ence in nonciliated cell volume density in the rats exposed for 3 months (3.42 ± 0.35), compared with those exposed for 20 months (2.58 ± 0.12) in the previous study, averaged over all exposure concentrations. In the caudal site, there was a statistically significant elevation in nonciliated cell volume density following exposure to 1.0 ppm ozone relative to both control and 0.12 ppm ozone.

The total epithelial volume density in the proximal bronchiole was greater in animals exposed for 3 months than in those exposed for 20 months (Table 4). Although the effect did not achieve significance, a similar trend was observed in the terminal bronchiole data.

VENTILATORY UNITS

Figure 4 illustrates an isolated ventilatory unit from a rat lung exposed to 1.0 ppm ozone for 3 months. For the epithelial, interstitial, capillary lumen, and alveolar macrophage compartments of the ventilatory unit, volume densities for each 100-μm interval (see Figure 2B) to 800 μm down the alveolar duct path are given in Tables 6 through 9. Multivariate analyses are presented in Table 10. Tables

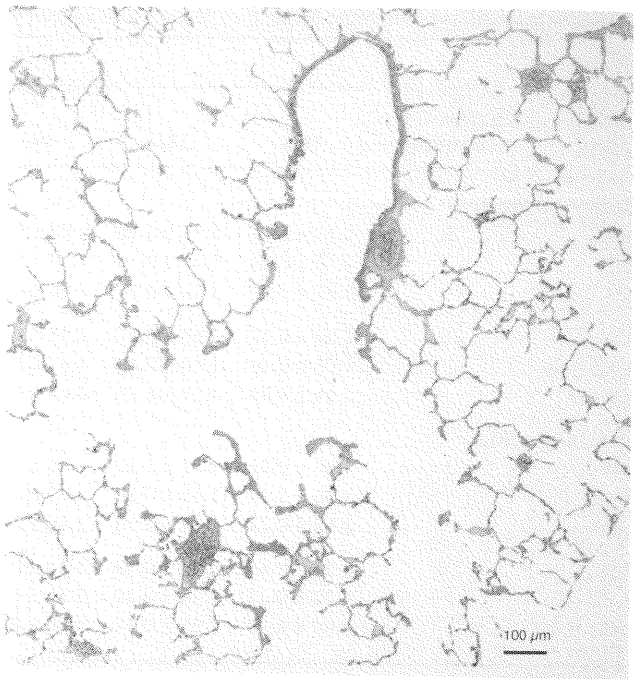

Figure 4. Ventilatory unit isolation from the lung of a rat exposed to 1.0 ppm ozone for 3 months.

Table 6. Total Epithelial Volume Density in Rats After Exposure to Ozone for 3 or 20 Months[a]

Ozone Concentration (ppm)	Length of Exposure (months)	Distance Down Alveolar Duct (μm)							
		100	200	300	400	500	600	700	800
Cranial Region									
0.0	3	0.82 ± 0.21	0.50 ± 0.10	0.26 ± 0.08	0.20 ± 0.03	0.22 ± 0.05	0.20 ± 0.04	0.13 ± 0.04	0.11 ± 0.06
0.12		1.27 ± 0.34	0.55 ± 0.12	0.30 ± 0.07	0.31 ± 0.03	0.22 ± 0.07	0.22 ± 0.06	0.30 ± 0.07	0.12 ± 0.04
1.0		3.02 ± 0.21	2.30 ± 0.44	1.05 ± 0.26	0.63 ± 0.14	0.47 ± 0.13	0.39 ± 0.09	0.24 ± 0.05	0.20 ± 0.06
0.0	20	2.03 ± 0.99	0.75 ± 0.38	0.13 ± 0.07	0.16 ± 0.03	0.08 ± 0.05	0.08 ± 0.03	0.02 ± 0.02	0.03 ± 0.03
0.12		2.21 ± 0.66	1.13 ± 0.27	0.61 ± 0.07	0.36 ± 0.14	0.61 ± 0.23	0.20 ± 0.11	0.34 ± 0.10	0.06 ± 0.03
1.0		3.15 ± 0.88	2.99 ± 0.83	2.92 ± 0.99	1.53 ± 0.57	1.60 ± 0.60	0.27 ± 0.13	0.46 ± 0.33	0.14 ± 0.09
Caudal Region									
0.0	3	1.02 ± 0.34	0.63 ± 0.23	0.25 ± 0.04	0.18 ± 0.04	0.18 ± 0.05	0.15 ± 0.02	0.10 ± 0.04	0.15 ± 0.05
0.12		1.25 ± 0.29	0.40 ± 0.12	0.32 ± 0.07	0.33 ± 0.09	0.31 ± 0.05	0.21 ± 0.06	0.22 ± 0.07	0.17 ± 0.06
1.0		2.99 ± 0.28	1.63 ± 0.27	1.35 ± 0.16	1.00 ± 0.16	0.51 ± 0.13	0.41 ± 0.15	0.29 ± 0.05	0.22 ± 0.06
0.0	20	1.27 ± 0.39	0.26 ± 0.17	0.40 ± 0.31	0.19 ± 0.07	0.08 ± 0.04	0.09 ± 0.05	0.12 ± 0.06	0.01 ± 0.01
0.12		1.55 ± 0.39	1.10 ± 0.36	0.65 ± 0.24	0.36 ± 0.17	0.28 ± 0.13	0.22 ± 0.11	0.39 ± 0.16	0.14 ± 0.04
1.0		2.25 ± 0.21	2.85 ± 0.33	1.29 ± 0.26	1.13 ± 0.27	0.91 ± 0.21	0.60 ± 0.34	0.16 ± 0.05	0.20 ± 0.11

[a] Values are presented as means ± SEM expressed as $\mu m^3/\mu m^2$; $n = 4$ for each ozone concentration group.

Table 7. Interstitial Volume Density in Rats After Exposure to Ozone for 3 or 20 Months[a]

Ozone Concentration (ppm)	Length of Exposure (months)	Distance Down Alveolar Duct (μm)							
		100	200	300	400	500	600	700	800
Cranial Region									
0.0	3	1.72 ± 0.19	1.74 ± 0.16	2.02 ± 0.17	1.94 ± 0.06	1.78 ± 0.18	1.93 ± 0.09	1.90 ± 0.18	1.58 ± 0.17
0.12		1.78 ± 0.09	1.58 ± 0.18	1.79 ± 0.10	1.62 ± 0.21	1.88 ± 0.18	1.50 ± 0.12	1.72 ± 0.14	1.45 ± 0.31
1.0		2.68 ± 0.30	3.38 ± 0.12	2.65 ± 0.13	2.08 ± 0.17	1.95 ± 0.19	1.99 ± 0.14	1.74 ± 0.22	1.62 ± 0.05
0.0	20	1.54 ± 0.32	1.68 ± 0.17	1.45 ± 0.23	1.27 ± 0.27	1.28 ± 0.06	1.84 ± 0.34	1.39 ± 0.15	1.54 ± 0.28
0.12		1.93 ± 0.20	1.58 ± 0.13	1.67 ± 0.34	1.41 ± 0.21	1.60 ± 0.20	1.43 ± 0.12	1.59 ± 0.28	1.52 ± 0.20
1.0		2.41 ± 0.46	4.12 ± 1.79	2.63 ± 0.24	2.11 ± 0.12	2.56 ± 0.30	1.56 ± 0.40	1.75 ± 0.47	1.19 ± 0.23
Caudal Region									
0.0	3	1.66 ± 0.22	1.71 ± 0.24	1.43 ± 0.17	1.74 ± 0.20	1.48 ± 0.17	1.55 ± 0.06	1.98 ± 0.37	1.20 ± 0.18
0.12		1.55 ± 0.17	1.55 ± 0.15	1.51 ± 0.16	1.70 ± 0.08	1.45 ± 0.09	1.49 ± 0.10	1.63 ± 0.09	1.74 ± 0.16
1.0		2.12 ± 0.23	2.71 ± 0.29	2.59 ± 0.18	2.48 ± 0.30	2.19 ± 0.21	2.14 ± 0.35	1.77 ± 0.15	1.68 ± 0.22
0.0	20	2.07 ± 0.41	1.50 ± 0.16	1.13 ± 0.12	1.36 ± 0.27	1.20 ± 0.10	1.61 ± 0.11	1.46 ± 0.29	1.15 ± 0.25
0.12		1.82 ± 0.33	1.74 ± 0.20	1.58 ± 0.19	1.62 ± 0.27	1.79 ± 0.17	1.54 ± 0.12	1.52 ± 0.13	1.26 ± 0.19
1.0		2.01 ± 0.16	1.82 ± 0.19	1.89 ± 0.23	2.44 ± 0.30	2.00 ± 0.09	1.59 ± 0.07	1.64 ± 0.46	1.90 ± 0.54

[a] Values are presented as means ± SEM expressed as $\mu m^3/\mu m^2$; $n = 4$ for each ozone concentration group.

Table 8. Capillary Lumen Volume Density in Rats After Exposure to Ozone for 3 or 20 Months[a]

Ozone Concentration (ppm)	Length of Exposure (months)	Distance Down Alveolar Duct (μm)							
		100	200	300	400	500	600	700	800
Cranial Region									
0.0	3	1.20 ± 0.20	1.33 ± 0.24	0.61 ± 0.19	1.05 ± 0.16	1.18 ± 0.10	1.17 ± 0.17	1.44 ± 0.34	1.13 ± 0.19
0.12		1.24 ± 0.24	1.23 ± 0.20	1.30 ± 0.18	1.22 ± 0.15	1.20 ± 0.14	1.17 ± 0.18	1.34 ± 0.17	1.18 ± 0.20
1.0		1.05 ± 0.16	1.07 ± 0.25	1.03 ± 0.26	0.98 ± 0.20	1.15 ± 0.19	1.34 ± 0.14	1.08 ± 0.34	1.20 ± 0.24
0.0	20	1.15 ± 0.13	1.67 ± 0.13	1.51 ± 0.37	1.92 ± 0.20	2.02 ± 0.37	1.75 ± 0.45	1.50 ± 0.06	1.54 ± 0.10
0.12		1.74 ± 0.26	1.92 ± 0.14	2.14 ± 0.30	1.52 ± 0.26	1.77 ± 0.19	1.49 ± 0.14	1.88 ± 0.40	1.94 ± 0.40
1.0		0.88 ± 0.36	0.86 ± 0.27	0.94 ± 0.21	1.87 ± 0.97	1.35 ± 0.34	1.71 ± 0.39	1.15 ± 0.16	1.56 ± 0.23
Caudal Region									
0.0	3	1.36 ± 0.10	1.19 ± 0.19	1.51 ± 0.08	1.50 ± 0.22	1.31 ± 0.16	1.38 ± 0.21	1.34 ± 0.22	1.02 ± 0.17
0.12		1.13 ± 0.26	1.43 ± 0.18	1.33 ± 0.22	1.26 ± 0.12	1.21 ± 0.16	1.24 ± 0.08	1.29 ± 0.08	1.12 ± 0.21
1.0		0.72 ± 0.11	0.90 ± 0.21	1.23 ± 0.16	1.13 ± 0.09	1.12 ± 0.20	1.10 ± 0.28	0.93 ± 0.10	1.13 ± 0.19
0.0	20	1.84 ± 0.53	1.87 ± 0.28	1.99 ± 0.47	1.67 ± 0.26	1.49 ± 0.22	2.02 ± 0.33	2.03 ± 0.20	1.38 ± 0.55
0.12		1.77 ± 0.19	1.78 ± 0.18	1.66 ± 0.26	1.94 ± 0.36	2.00 ± 0.24	2.10 ± 0.17	1.63 ± 0.28	1.88 ± 0.29
1.0		0.97 ± 0.24	1.14 ± 0.22	1.15 ± 0.29	1.40 ± 0.32	1.47 ± 0.27	1.49 ± 0.29	1.72 ± 0.20	2.49 ± 0.69

[a] Values are presented as means ± SEM expressed as $\mu m^3/\mu m^2$; $n = 4$ for each ozone concentration group.

Table 9. Macrophage Volume Density in Rats After Exposure to Ozone for 3 or 20 Months[a]

Ozone Concentration (ppm)	Length of Exposure (months)	Distance Down Alveolar Duct (μm)							
		100	200	300	400	500	600	700	800
Cranial Region									
0.0	3	0.07 ± 0.04	0.11 ± 0.03	0.12 ± 0.06	0.07 ± 0.03	0.12 ± 0.04	0.13 ± 0.05	0.05 ± 0.04	0.03 ± 0.03
0.12		0.07 ± 0.02	0.08 ± 0.02	0.09 ± 0.03	0.10 ± 0.03	0.12 ± 0.05	0.09 ± 0.04	0.09 ± 0.05	0.02 ± 0.02
1.0		0.23 ± 0.10	0.25 ± 0.04	0.23 ± 0.07	0.13 ± 0.03	0.12 ± 0.05	0.18 ± 0.09	0.09 ± 0.02	0.10 ± 0.03
0.0	20	0.00 ± 0.00	0.01 ± 0.01	0.04 ± 0.04	0.02 ± 0.02	0.04 ± 0.02	0.00 ± 0.00	0.07 ± 0.07	0.00 ± 0.00
0.12		0.16 ± 0.10	0.04 ± 0.03	0.12 ± 0.03	0.03 ± 0.03	0.04 ± 0.04	0.05 ± 0.02	0.08 ± 0.02	0.00 ± 0.00
1.0		0.07 ± 0.04	0.07 ± 0.07	0.10 ± 0.06	0.06 ± 0.04	0.10 ± 0.10	0.04 ± 0.04	0.21 ± 0.04	0.00 ± 0.00
Caudal Region									
0.0	3	0.03 ± 0.02	0.07 ± 0.03	0.01 ± 0.01	0.07 ± 0.02	0.10 ± 0.05	0.12 ± 0.06	0.09 ± 0.03	0.15 ± 0.09
0.12		0.07 ± 0.02	0.13 ± 0.04	0.10 ± 0.06	0.09 ± 0.03	0.05 ± 0.03	0.17 ± 0.03	0.05 ± 0.02	0.05 ± 0.02
1.0		0.22 ± 0.07	0.38 ± 0.13	0.32 ± 0.06	0.27 ± 0.03	0.40 ± 0.04	0.27 ± 0.05	0.09 ± 0.04	0.13 ± 0.05
0.0	20	0.00 ± 0.00	0.01 ± 0.01	0.00 ± 0.00	0.01 ± 0.01	0.08 ± 0.06	0.05 ± 0.03	0.00 ± 0.00	0.00 ± 0.00
0.12		0.09 ± 0.03	0.04 ± 0.01	0.07 ± 0.02	0.07 ± 0.02	0.02 ± 0.02	0.04 ± 0.03	0.03 ± 0.02	0.03 ± 0.02
1.0		0.17 ± 0.03	0.27 ± 0.11	0.21 ± 0.08	0.29 ± 0.15	0.11 ± 0.05	0.06 ± 0.04	0.00 ± 0.00	0.00 ± 0.00

[a] Values are presented as means ± SEM expressed as $\mu m^3/\mu m^2$; $n = 4$ for each ozone concentration group.

11 and 12 provide ANOVA p values and subtest results (least squares means), respectively, for total epithelial volume density. Tables 13 and 14 give ANOVA p values and subtest results for interstitial and macrophage volume density, respectively. Figures 5 through 8 are line graphs to illustrate epithelial, interstitial, capillary lumen, and macrophage volume density, respectively, as a function of distance down the alveolar duct path.

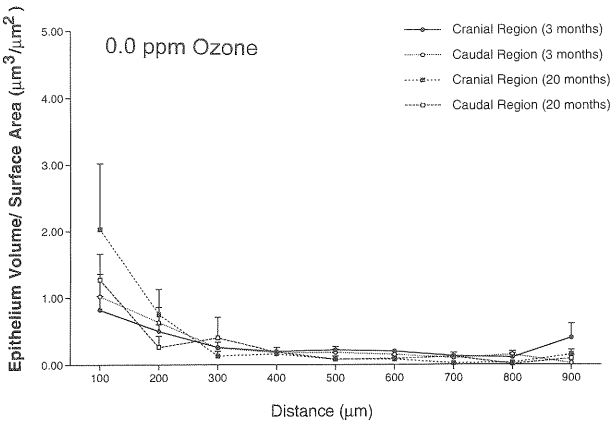

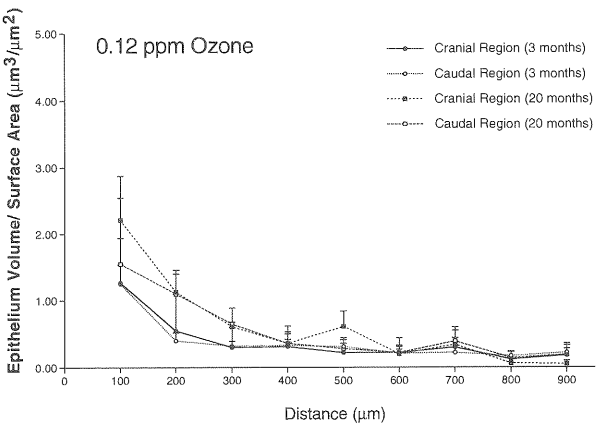

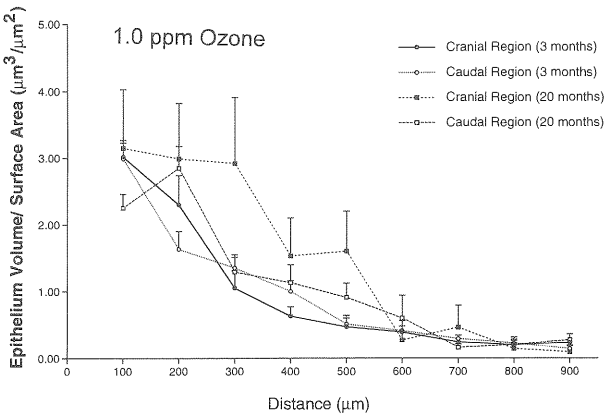

Figure 5. Epithelial volume density of the alveolar septa expressed as a function of distance down the alveolar duct path of the ventilatory units in the cranial and caudal regions of rats exposed to 0.0, 0.12, or 1.0 ppm ozone for 3 or 20 months.

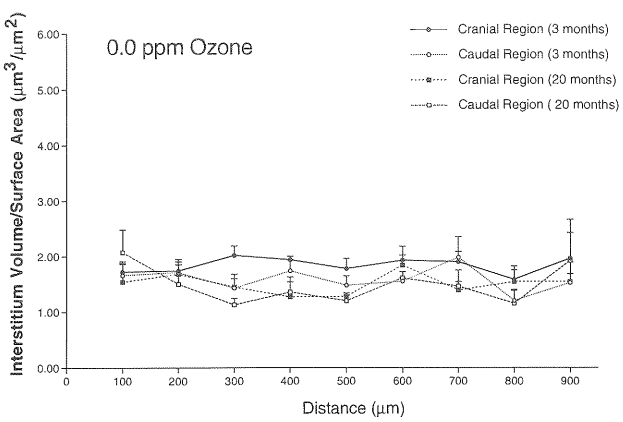

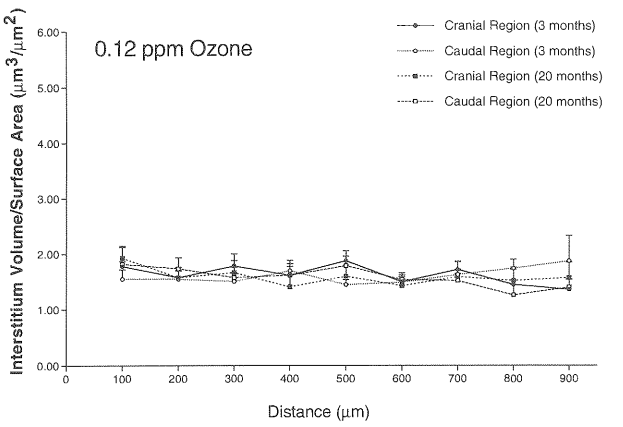

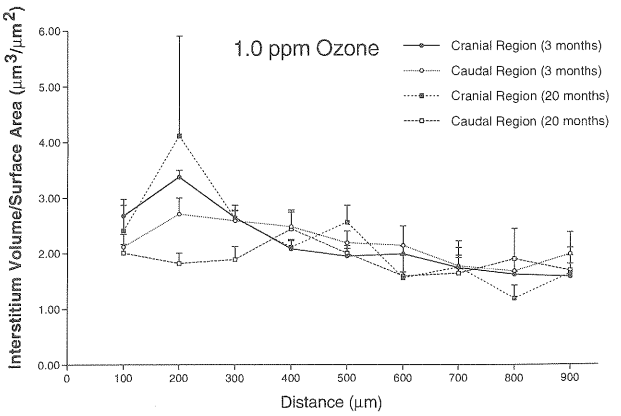

Figure 6. Interstitial volume density of the alveolar septa expressed as a function of distance down the alveolar duct path of the ventilatory units in the cranial and caudal regions of rats exposed to 0.0, 0.12, or 1.0 ppm ozone for 3 or 20 months.

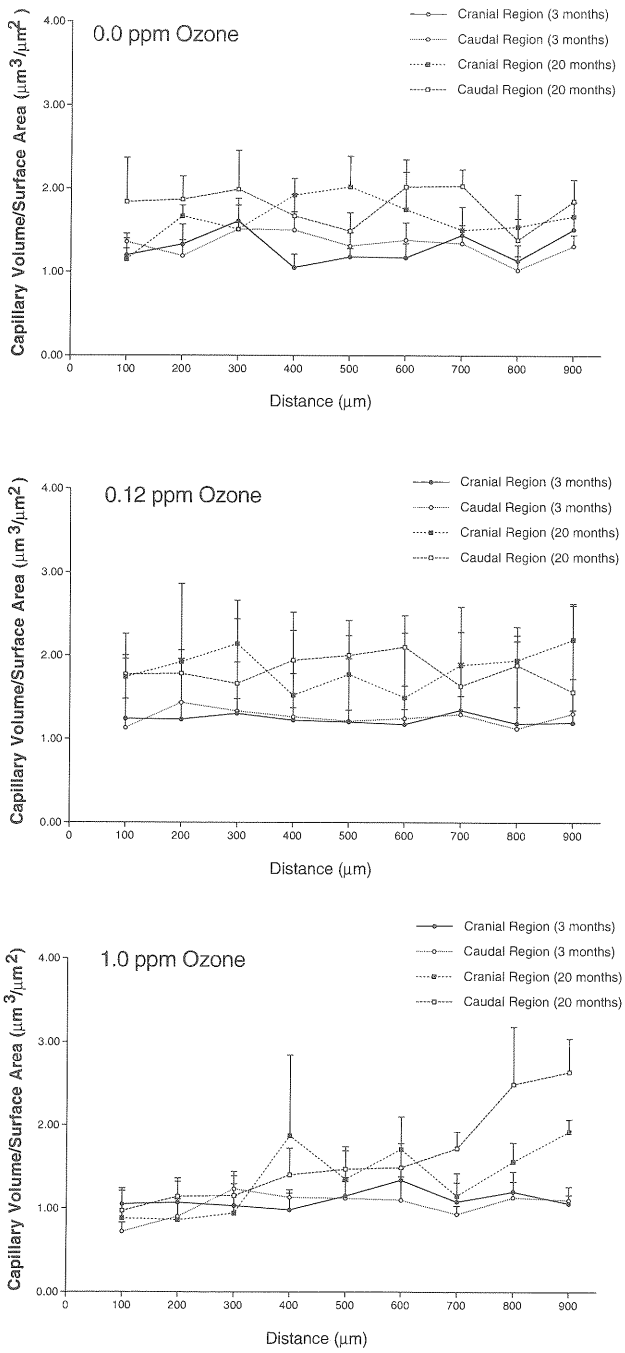

Figure 7. Capillary lumen volume density of the alveolar septa expressed as a function of distance down the alveolar duct path of the ventilatory units in the cranial and caudal regions of rats exposed to 0.0, 0.12, or 1.0 ppm ozone for 3 or 20 months.

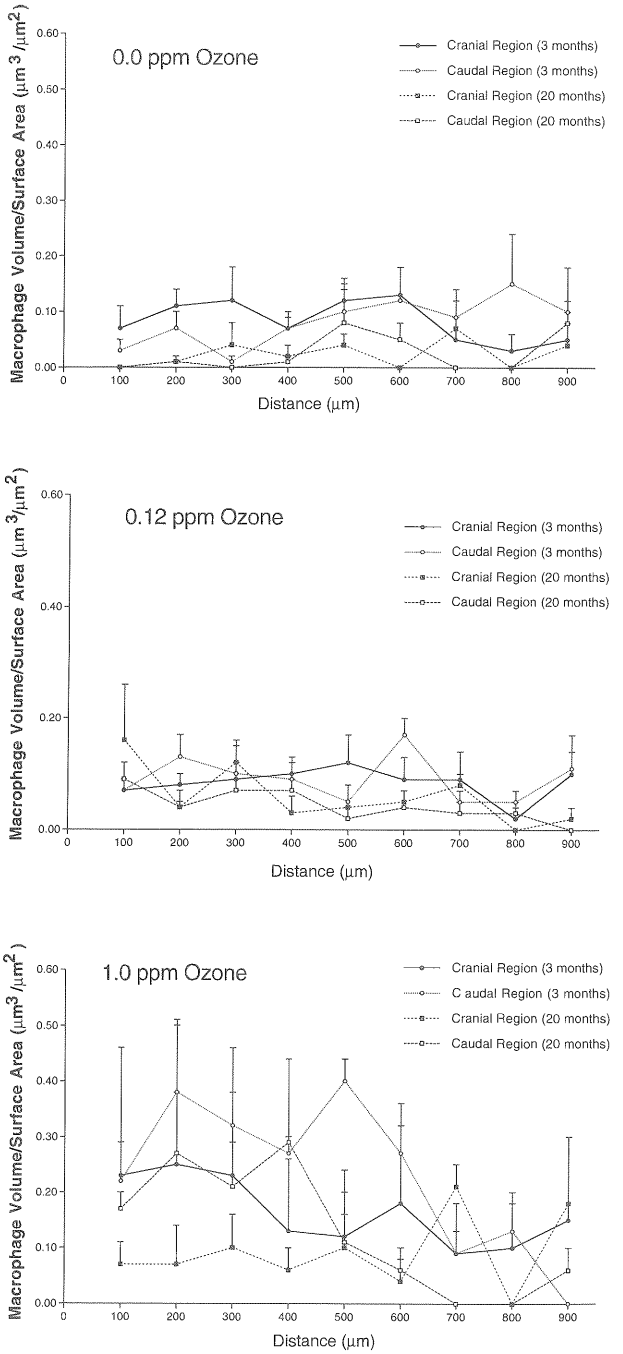

Figure 8. Alveolar macrophage volume density within the alveolar airspaces expressed as a function of distance down the alveolar duct path of the ventilatory units in the cranial and caudal regions of rats exposed to 0.0, 0.12, or 1.0 ppm ozone for 3 or 20 months.

Total Epithelial Volume Density

Statistically significant differences between the cranial and caudal sites for the vector of epithelial volume density estimated parameters were found, so the parameter vectors were analyzed separately for the two sites (Table 10). In the cranial site a significant multivariate effect was found for the interaction between concentration and time. Significant interactions were found for individual ANOVAs for SSE and A3 (the volume density of the epithelium in the distal region of the ventilatory unit). Significant effects of length of exposure and of ozone exposure concentration were observed for the volume density of the epithelium (A0), the distance into the ventilatory unit for which this volume density was observed (X1), and the distance into the ventilatory unit at which the volume density decreased to its lower value (X2) (Table 11). The subtests are presented in Table 12 and show an increasing effect as a function of increasing ozone exposure concentration for both 3- and

Table 10. *p* Values from Multivariate Analyses of Variance[a]

	Dependent Variable Vector			
Analysis and Factor	Expressed as Difference Between Cranial and Caudal Sites[b]	Expressed as Average of Cranial and Caudal Sites[b]	For the Cranial Site	For the Caudal Site
Repeated Measures[c]				
Interstitial Volume Density				
Distance	0.10		0.02	0.13
Distance × time	0.79		0.65	0.63
Distance × concentration	0.02*		< 0.01*	0.09
Distance × concentration × time	0.14		0.30	0.36
Macrophage Volume Density				
Distance	0.16	< 0.01		
Distance × time	0.52	0.09		
Distance × concentration	0.63	< 0.01*		
Distance × concentration × time	0.26	0.52		
Capillary Lumen Volume Density				
Distance	0.95	0.60		
Distance × time	0.13	0.25		
Distance × concentration	0.56	0.15		
Distance × concentration × time	0.28	0.75		
MANOVAs[d]				
Total Epithelial Volume Density				
Time	< 0.01		< 0.01	0.14
Concentration	< 0.01		< 0.01	< 0.01*
Concentration × time	< 0.01*		< 0.01*	0.87

[a] The *p* values correspond to the *F* test using the Hotelling-Lawley trace. An effect was considered significant if $p < 0.05$. An asterisk (*) indicates a significant effect that determined the next level of analysis.

[b] Significant effects in any of the factors for the analysis in which the dependent variable vector was expressed as the difference between the cranial and caudal sites resulted in separate analyses for the two sites. If no statistically significant effects were observed, the values were averaged before analysis.

[c] The dependent variable vector for interstitial, macrophage, and capillary lumen volume density repeated measures analyses consisted of the eight distance intervals down the alveolar duct.

[d] The dependent variable vector for the epithelial volume density MANOVA consisted of the five estimated parameters (A0, A3, X1, X2, B2) and the SSE.

Table 11. Total Epithelial Volume Density: ANOVA *p* Values[a]

	ANOVA Dependent Variable					
Factor	SSE	A0	A3	X1	X2	B2
Cranial Site						
Time	0.02	< 0.01*	0.03	< 0.01*	0.03*	0.37
Concentration	0.01	< 0.01*	0.04	< 0.01*	< 0.01*	0.46
Concentration × time	0.01*	0.96	0.02*	0.37	0.50	0.80
Caudal Site						
Concentration[b]	0.02*	< 0.01*	0.03*	0.66	< 0.01*	< 0.01*

[a] The *p* values correspond to the individual factor tests from the ANOVA. An effect was considered significant if $p < 0.05$. An asterisk (*) indicates a significant effect that determined the next level of analysis.

[b] The factor for the caudal site consists only of concentration because no time effects were significant at the multivariate level of testing (see Table 10).

Table 12. Total Epithelial Volume Density: Least Squares Means[a]

Ozone Concentration (ppm)	Length of Exposure (months)	Parameter[bc]					
		SSE	A0	A3	X1	X2	B2
Cranial Site							
0.0	3	0.28 ± 0.35[b]	0.82 ± 0.50[b]	0.26 ± 0.04[b]	41 ± 28[b]	128 ± 52[b]	−2.0 ± 0.4[b]
0.12		0.22 ± 0.32[b]	1.44 ± 0.46[b]	0.26 ± 0.04[b]	65 ± 25[bc]	155 ± 47[b]	−2.1 ± 0.4[b]
1.0		0.26 ± 0.35[b]	3.58 ± 0.50[c]	0.31 ± 0.04[b]	137 ± 28[c]	379 ± 52[c]	−1.4 ± 0.4[b]
0.0	20	0.05 ± 0.39[b]	2.27 ± 0.56[b]	0.09 ± 0.05*[b]	78 ± 31[b]	190 ± 58[b]	−2.3 ± 0.4[b]
0.12		0.66 ± 0.39[b]	2.96 ± 0.56[b]	0.33 ± 0.05[c]	134 ± 31[b]	227 ± 58[b]	−2.1 ± 0.4[b]
1.0		2.41 ± 0.39*[c]	5.31 ± 0.56*[c]	0.14 ± 0.05*[b]	257 ± 31*[c]	560 ± 58*[c]	−2.0 ± 0.4[b]
Caudal Site							
0.0	3	0.23 ± 0.22	1.21 ± 0.42	0.19 ± 0.06	59 ± 29	153 ± 49	−2.0 ± 0.2
0.12		0.19 ± 0.20	1.25 ± 0.38	0.28 ± 0.06	60 ± 26	148 ± 44	−2.0 ± 0.2
1.0		0.62 ± 0.22	2.79 ± 0.42	0.32 ± 0.06	53 ± 29	456 ± 48	−0.9 ± 0.2
0.0	20	0.37 ± 0.25	1.51 ± 0.47	0.14 ± 0.07	76 ± 32	166 ± 54	−2.0 ± 0.2
0.12		0.32 ± 0.22	2.08 ± 0.42	0.27 ± 0.06	117 ± 29	268 ± 49	−1.5 ± 0.2
1.0		1.25 ± 0.25	3.46 ± 0.47	0.39 ± 0.07	150 ± 32	469 ± 54	−1.0 ± 0.2
0.0	Average	0.29 ± 0.17[b]	1.34 ± 0.32[b]	0.17 ± 0.05[b]	67 ± 23[b]	159 ± 36[b]	−2.0 ± 0.2[b]
0.12		0.25 ± 0.15[b]	1.62 ± 0.29[b]	0.27 ± 0.04[bc]	86 ± 21	203 ± 33[b]	−1.8 ± 0.1[b]
1.0		0.90 ± 0.17[c]	3.09 ± 0.32[c]	0.35 ± 0.05[c]	96 ± 23[b]	462 ± 36[c]	−0.9 ± 0.2[c]

[a] Least squares means ± SE are reported separately for the two exposure times as well as pooled over exposure times (average) for the caudal site. For the cranial site, subtests (uncorrected *t* tests) were performed only for separate exposure times (3 or 20 months). For the caudal site, subtests (uncorrected *t* tests) were performed only for the pooled exposure times. An asterisk (*) indicates a significant ($p < 0.05$) difference between 3 and 20 months of exposure for a given exposure concentration.

[bc] For a given parameter, all concentration means identified by the same letter (b, for example) were not significantly different from one another; means identified by different letters (b and c) were significantly different from one another. A column with no means identified with a letter indicates no significant effects of ozone concentration in that parameter.

20-month exposures. However, it was only following the 1.0 ppm exposure concentration that the differences were statistically significant relative to control parameters. Additionally, the changes were always greatest in the animals exposed to 1.0 ppm ozone for 20 months when compared either with the other groups exposed for 20 months or with those animals exposed to 1.0 ppm ozone for 3 months.

In the caudal region, no statistically significant multivariate differences with length of exposure were observed and subtests were performed only for concentration effects. As for the cranial region, statistically significant changes were found only for rats exposed to 1.0 ppm ozone despite trends consistent with the increasing ozone exposure concentration.

Interstitial Volume Density

Statistically significant differences in interstitial volume density were found between the cranial and caudal sites (Table 10). In the cranial site, the concentration-related changes in the interstitial volume density were observed for the first 500 μm into the ventilatory unit. Although the mean values decreased in an essentially monotonic fashion following 0.12 ppm ozone, the differences were pronounced and statistically significant only following exposure to 1.0 ppm ozone (Table 13). In the caudal site, interstitial volume density did not change as a function of distance, so the values were averaged to create a single value for each animal. In the caudal site also, no statistically significant differences associated with length of exposure were observed. A significant elevation in volume density was observed following exposure to 1.0 ppm ozone.

Capillary Lumen Volume Density

No significant differences between the cranial and caudal sites were observed for capillary lumen volume density (Table 10), nor were effects observed related to distance when analyzed as the averaged values. A single ANOVA averaged over distance and over the two sites was con-

Table 13. Interstitial Volume Density: Least Squares Means[a]

Ozone Concentration (ppm)	Length of Exposure (months)	Distance Down Alveolar Duct[bc] (μm)								
		100	200	300	400	500	600	700	800	Pooled
Cranial Site										
0.0	Average	1.86 ± 0.19^{b}	1.60 ± 0.16^{b}	1.28 ± 0.13^{b}	1.55 ± 0.17^{b}	1.34 ± 0.11^{b}	1.58 ± 0.12	1.72 ± 0.19	1.17 ± 0.19	
0.12		1.68 ± 0.17^{b}	1.65 ± 0.14^{b}	1.54 ± 0.12^{b}	1.66 ± 0.16^{bc}	1.62 ± 0.10^{bc}	1.51 ± 0.12	1.57 ± 0.17	1.50 ± 0.17	
1.0		2.06 ± 0.19^{c}	2.27 ± 0.16^{c}	2.24 ± 0.13^{c}	2.46 ± 0.17^{c}	2.10 ± 0.11^{c}	1.86 ± 0.13	1.71 ± 0.19	1.79 ± 0.19	
Caudal Site										
0.0	3									1.59 ± 0.11
0.12										1.58 ± 0.10
1.0										2.21 ± 0.11
0.0	20									1.44 ± 0.12
0.12										1.61 ± 0.11
1.0										1.91 ± 0.12
0.0	Average									1.51 ± 0.08^{b}
0.12										1.59 ± 0.07^{b}
1.0										2.06 ± 0.08^{c}

[a] Least squares means ± SE are reported. Comparisons are among ozone exposure groups for a given distance interval. Subtests were uncorrected *t* tests.

[bc] For a given distance interval, all concentration means identified by the same letter (b, for example) were not significantly different from one another; means identified by different letters (b and c) were significantly different from one another. A column in which no means are identified with a letter indicates no significant effects of ozone concentration were found in that parameter.

ducted. A significant time effect ($p < 0.01$) was found with capillary lumen volume density being significantly greater in rats exposed for 20 months (1.63 ± 0.09) than in rats exposed for 3 months (1.20 ± 0.08).

Macrophage Volume Density

No significant differences between macrophage volume density at the cranial and caudal sites were observed (Table 10). The data were averaged for subsequent analyses. A significant concentration × distance interaction was tested by examining the concentration effects from the individual distance interval ANOVAs. These results (Table 14) indicated a signficant elevation in macrophage volume density following exposure to 1.0 ppm ozone for either 3 or 20 months through the first 500 μm of the ventilatory unit.

ANTIOXIDANT ENZYME LOCALIZATION

We examined rat lungs exposed to ozone for 2 months to identify Cu-Zn SOD and Mn SOD. Slices through the left lobe of rat lungs exposed to 0.0 or 1.0 ppm ozone were analyzed to determine the distribution and relative abundance of these two antioxidant enzymes and any changes associated with ozone exposure. Cu-Zn SOD was found in the airways down to the level of the terminal bronchioles. Virtually all cells of the upper airways were labeled and, of these, mainly Clara cells were labeled at the level of the terminal bronchiole. Fibroblasts and alveolar macrophages were labeled in the parenchyma with type II epithelial cells labeled occasionally. The labeling of Cu-Zn SOD in airway cells and the distal parenchyma was markedly reduced by ozone exposure (Figure 9A and B), with retention of label in the pleura, the region of the lung that receives the lowest dose of ozone from an exposure. Ozone exposure reduced both the intensity and extent of labeling in the parenchyma and the airways (Figure 9A and B) with retention of label in the pleura (data not shown). When the dilution of Cu-Zn SOD antibody was changed from 1:10,000 to 1:100,000, the labeling in the parenchyma was lost. Light labeling of the airways in ozone-exposed animals was evident, while a heavier degree of labeling over the airways in control animals was noted. Therefore the density of Cu-Zn SOD in tissues was higher in the airways than in the parenchyma of the lung in control animals and was reduced by ozone exposure. These distinctions were enhanced after we used high dilutions of the antisera.

Mn SOD labeled the pleura lightly and labeled the airways moderately down to the level of terminal bronchioles. In terminal bronchioles, Clara cells were the primary cell type to show labeling for Mn SOD. Alveolar macrophages and type II epithelial cells were heavily labeled in the proximal alveolar duct regions (Figure 9C and D). Ozone exposure caused an increase in labeling of type II epithelial cells (Figure 9E and F) in the proximal alveolar ducts. Alveolar macrophages, which increased in number with ozone exposure, were heavily labeled and thus contributed to the overall increase in Mn SOD in the proximal alveolar region (Figure 9E and F).

The primary target for ozone damage in the lung, the bronchiole-alveolar duct region, was further studied with methods more sensitive to changes in antioxidant enzymes on a per-cell basis. Mn and Cu-Zn SOD were studied by means of protein A gold immunolabeling at the electron microscopic level, which is a sensitive, quantitative method

Table 14. Macrophage Volume Density: ANOVA p Values and Subtests

	Distance Down Alveolar Duct (μm)							
	100	200	300	400	500	600	700	800
ANOVA p Value[a] for Dependent Variable								
Concentration	< 0.01*	< 0.01*	< 0.01*	< 0.01*	< 0.01*	0.29	0.18	0.39
Least Squares Means[b] for Ozone Concentration (ppm)								
0.0	0.03 ± 0.03[c]	0.06 ± 0.03[c]	0.04 ± 0.03[c]	0.05 ± 0.02[c]	0.09 ± 0.02[c]	0.08 ± 0.03	0.06 ± 0.02	0.06 ± 0.02
0.12	0.09 ± 0.02[c]	0.08 ± 0.03[c]	0.09 ± 0.03[c]	0.08 ± 0.02[c]	0.06 ± 0.02[c]	0.09 ± 0.03	0.06 ± 0.01	0.03 ± 0.02
1.0	0.18 ± 0.03[d]	0.25 ± 0.03[d]	0.22 ± 0.03[d]	0.19 ± 0.02[d]	0.19 ± 0.02[d]	0.15 ± 0.03	0.10 ± 0.02	0.07 ± 0.02

[a] The p values correspond to the individual factor test for concentration from the ANOVAs for the distance intervals. The data from the cranial and caudal sites were averaged to perform this analysis. An effect was considered significant if $p < 0.05$. An asterisk (*) indicates a significant effect that determined the next level of analysis.

[b] Least squares means ± SE are reported. Subtests were uncorrected t tests. For a given distance interval, all concentration means identified by the same letter (c, for example) were not significantly different from one another; means identified by different letters (c and d) were significantly different from one another. A column in which no means are identified with a letter indicates no significant effects of ozone concentration were found in that parameter.

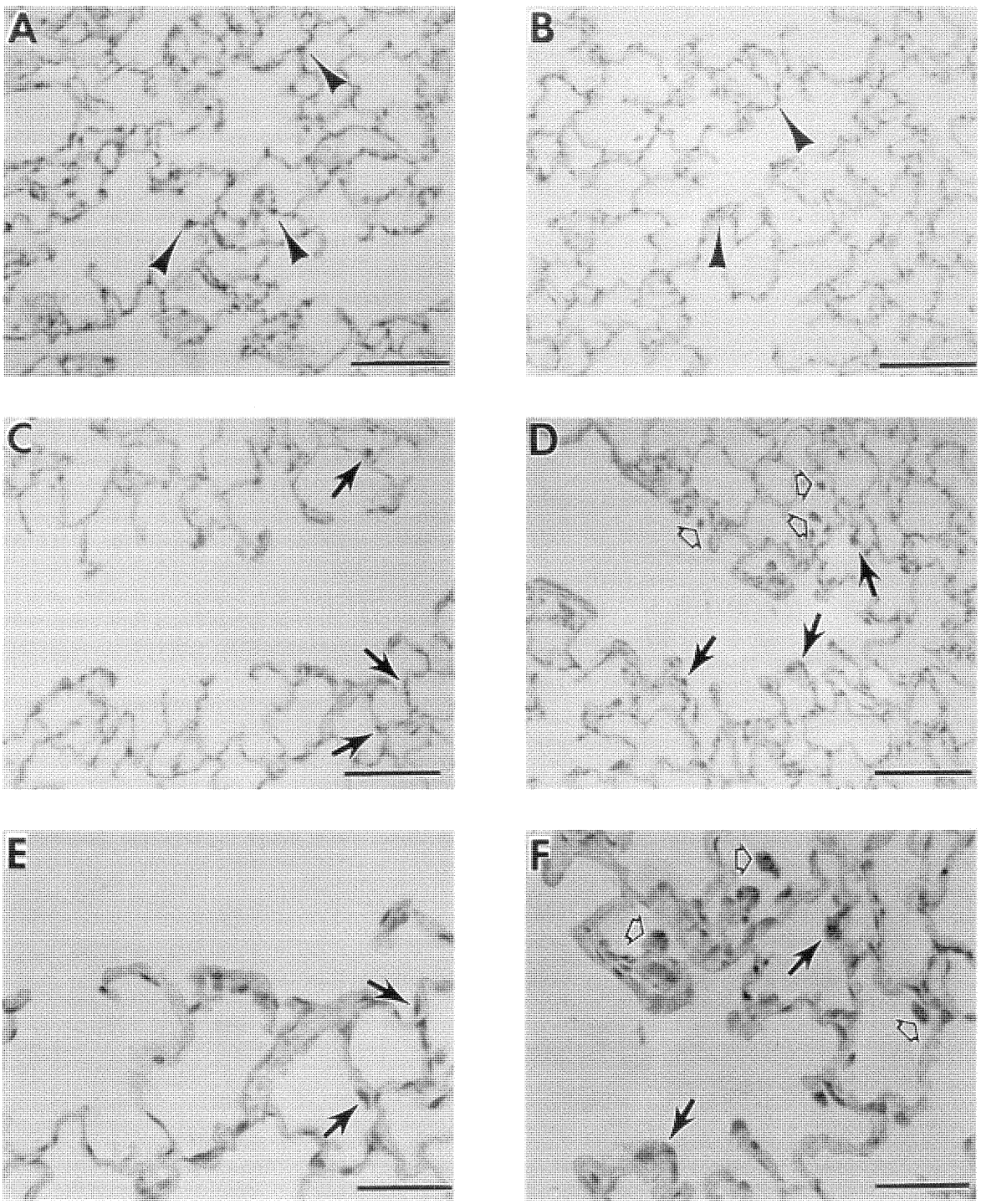

Figure 9. The distribution of Cu-Zn SOD and Mn SOD in rat lungs exposed to 0.0 (control) or 1.0 ppm ozone for 2 months shown by using immunohistochemistry. (A) A control rat lung labeled for Cu-Zn SOD (dilution 1:10,000). Dense labeling is noted in the parenchyma (arrowheads). (B) An exposed rat lung labeled for Cu-Zn SOD (dilution 1:10,000). A general reduction of labeling density is noted in the distal parenchyma (arrowheads). (C) A control rat lung labeled for Mn SOD (dilution 1:1,000). Few labeled type II epithelial cells are noted in the proximal alveolar region (long arrow). (D) An exposed rat lung labeled for Mn SOD (dilution 1:1,000). Increased labeling of type II alveolar epithelial cells (long arrows) and alveolar macrophages (open arrows) is seen in the proximal alveolar region. (E) A higher magnification of panel C, a control rat lung proximal alveolar region, with few labeled type II epithelial cells (long arrows). (F) A higher magnification of panel D, an exposed rat lung, that more clearly details the increase in labeling of type II epithelial cells (long arrows) and alveolar macrophages (open arrows). Bars = 100 μm for panels A, B, C, and D, and 50 μm for panels E and F.

for assessing changes in SOD with ozone exposure. Both Mn and Cu-Zn SOD were studied in terminal bronchioles and the alveolar duct regions in animals exposed to 0.0 or 1.0 ppm ozone for 2 months. Mn SOD was examined in the Clara cells of terminal bronchioles in animals exposed to 0.0 or 1.0 ppm ozone and was not found to increase as a result of ozone exposure (Figure 10). Prolonged exposure to higher levels of ozone has been found to result in a bronchiolarized metaplasia of the epithelium of the alveolar ducts with a change in cell type from the usual type I and type II epithelium into a cuboidal epithelium composed of Clara cells, ciliated cells, and undifferentiated cuboidal cells (Pinkerton et al. 1993, 1995). We also found evidence of bronchiolarized metaplasia in alveolar ducts of animals exposed to 1.0 ppm ozone for 2 months. The bronchiolarized metaplasia was confined to the proximal alveolar region within 200 μm of a terminal bronchiole (Figure 11A). The Clara cells found in the bronchiolarized portions of alveolar ducts as a result of ozone exposure demonstrated the same relative degree of labeling for Mn SOD as did Clara cells in the terminal bronchioles in both ozone-exposed and control animals (Figure 10). Bronchiolarized metaplasia was not found in alveolar ducts of control animals (Figure 11B).

The expression of Mn SOD in type II epithelial cells was studied in two locations along alveolar ducts: 0 to 400 μm from the BADJ and the distal parenchyma located further than 600 μm from the BADJ (Table 15). As with all cell types studied, labeling was mainly confined to the mitochondria of the cells with only minimal background labeling of the cytoplasm (Figure 12). The labeling for Mn SOD was significantly increased in type II epithelial cells located 0 to 400 μm from the BADJ in animals exposed for 2 months to 1.0 ppm ozone (Figure 13). With increased distance down the alveolar ducts, in regions farther than 600 μm from the BADJ, the level of Mn SOD labeling was not significantly changed from control values (Figure 13). The increase in Mn SOD in the proximal alveolar region was unrelated to the density of mitochondria in type II epithelial cells, as cell-specific mitochondrial density did not change with changing distance from the BADJ (Table 16). In addition to the changes in the epithelial cells, interstitial fibroblasts

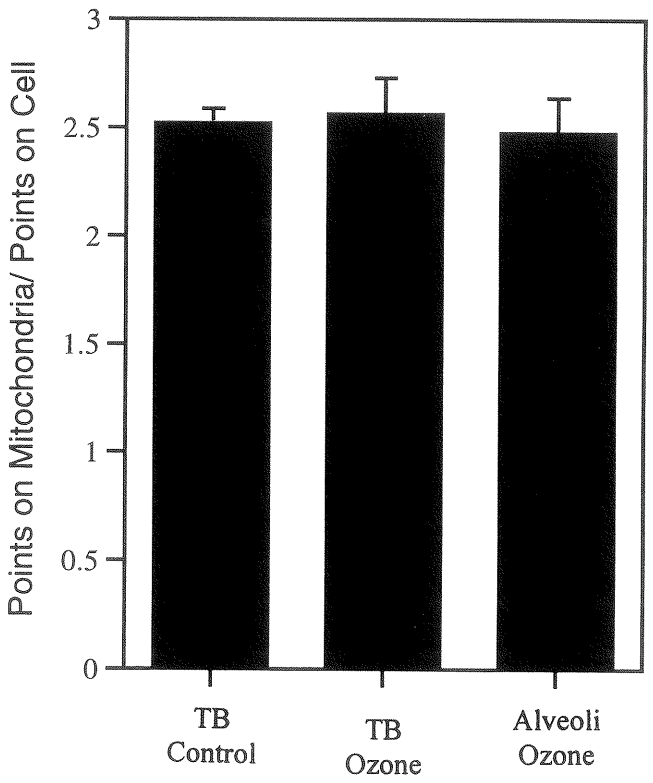

Figure 10. The level of Mn SOD in the Clara cells of the terminal bronchioles (TB) and alveolar duct regions in rat lungs exposed to 0.0 or 1.0 ppm ozone for 2 months. All data are means ± SEM. No significant differences were noted using Student's *t* test.

Figure 11. The BADJ of rat lungs exposed to 0.0 or 1.0 ppm ozone for 2 months. (A) Terminal bronchiole (arrowheads) and alveolar duct region of an exposed rat lung. An area of bronchiolarized metaplasia (long arrows) is seen as well as clusters of alveolar macrophages (open arrows). (B) Terminal bronchiole (arrowheads) and alveolar duct region of a control rat lung. Bars = 50 μm.

were studied for induction of Mn SOD. No induction was found in interstitial fibroblasts located in alveolar ducts (Table 15). Thus, the major site of induction of Mn SOD was in the proximal portions of the gas exchange region, and this induction occurred specifically in the mitochondria of type II alveolar epithelial cells.

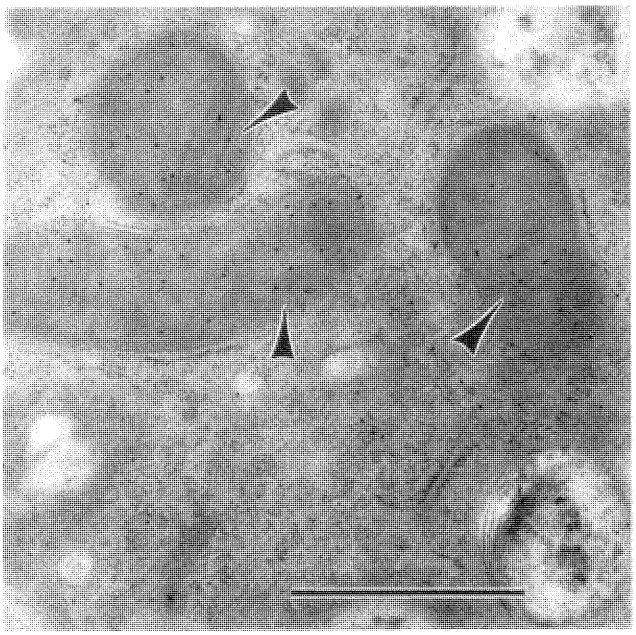

Figure 12. Electron micrograph of a type II epithelial cell from a rat lung exposed to 1.0 ppm ozone for 2 months and immunolabeled for Mn SOD with protein A-gold. Gold grains can be seen labeling Mn SOD in the mitochondria (arrowheads). Bar = 1 μm.

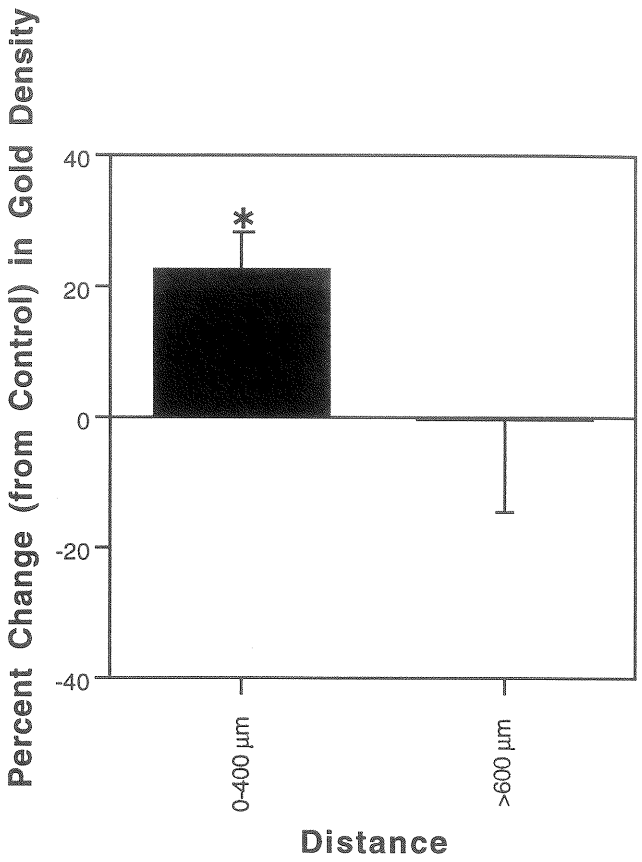

Figure 13. The percentage of change from control in Mn SOD levels in type II alveolar epithelial cells as a function of distance from the BADJ. The animals were exposed to either 0.0 or 1.0 ppm ozone for 2 months. Mn SOD expression was measured in a proximal location 0 to 400 μm from the BADJ, and in the distal parenchyma located farther than 600 μm from the BADJ. All data are means ± SEM. An asterisk (*) indicates a significant ($p < 0.05$) change from control levels using Student's t test.

Table 15. The Level of Mn SOD in Type II Epithelial Cells, Interstitial Fibroblasts, and Clara Cells[a]

Distance from BADJ	Type II Epithelial Cells		Fibroblasts		Clara Cells		
	Control	Ozone	Control	Ozone	Location	Control	Ozone
0–400 μm	3.324 ± 0.217	4.037 ± 0.092[b]	3.405 ± 0.335	3.659 ± 0.408	Terminal bronchiole	2.522 ± 0.065	2.565 ± 0.165
> 600 μm	3.54 ± 0.512	3.322 ± 0.137	NA[c]	NA	Alveolus	—	2.477 ± 0.134

[a] Data reflect the number of gold particles per number of points on mitochondria, and are expressed as means ± SEM.

[b] $p < 0.05$ compared with control cells using Student's t test.

[c] NA = not available.

Table 16. Density of Mitochondria in Type II Epithelial Cells[a]

Distance from BADJ	Control	Ozone
0–400 μm	0.196 ± 0.016	0.177 ± 0.021
> 600 μm	0.138 ± 0.019	0.140 ± 0.005

[a] Data are the points on mitochondria per points on type II epithelial cells, and are expressed as means ± SEM.

DISCUSSION

TRACHEOBRONCHIAL AIRWAYS

Epithelial reorganization of the airways plays an important role in the development of tolerance produced by long-term exposure to ozone. The changes vary according to site and are most pronounced in those portions of the tracheobronchial tree that are most affected in short-term exposures. Some changes appear to be dose-dependent, whereas others are not. These changes predominantly involve alterations in the cellular composition of the epithelial lining. The most significant effects within the airways due to progressive exposure to ozone were obvious only in rats exposed to 1.0 ppm ozone.

The natural aging process of rats does not play a significant role in the ozone-induced effects observed after 20 months of exposure. We calculated volume densities for several types of cells to determine the total volume densities of the epithelial and interstitial tissue compartments within ventilatory units in the cranial and caudal portions of the lung as functions of distance from the BADJ. Measurements expressed in this context showed no significant increase in the volumes of these tissue compartments between 3 and 20 months of age. This finding helps to rule out aging as a contributor to the effects observed in the lungs of F344/N rats after 20 months of exposure to ozone.

The variability in epithelial response observed in different regions of the tracheobronchial airways is consistent with predictions of local ozone dose based on computer simulation models (Overton et al. 1987, 1989; Miller et al. 1988). These models, which take into account differences in path length from the trachea to the terminal bronchiole, predict differences in the amount of ozone delivered to different sites within the tracheobronchial airways (Overton et al. 1989). Simplifying the assumptions used in these models, it can be shown that delivered dose depends primarily on transit time and distal volume. The test sites selected in this study allow qualitative examination of the relative importance of transit time (approximated by path length) and distal volume (estimated from the data of Raabe and associates (1976).

VENTILATORY UNITS

The reorganization of the centriacinar region of the lung is a well-recognized result of continued inhalation of toxic oxidant gases at high ambient levels. Previous work has shown that reasonably long-term (2- to 3-month) exposure to oxidant air pollutants, such as ozone and nitrogen dioxide, alters the mixture of epithelial cell populations that occupy the proximal gas exchange areas of pulmonary acini in species with short or nonexistent respiratory bronchioles (Boorman et al. 1980; Barr et al. 1988, 1990). The present study expands these observations and addresses some of the questions raised by these previous investigations. What is the extent of the reorganized proximal alveolar ducts at different concentrations of ozone at different times during the course of ozone exposure? When comparing ozone exposures of 3 and 20 months' duration, how heterogeneous is the extent of this reorganization within the centriacinar region of the same animal or between animals at different concentrations of ozone? Is the degree of differentiation of the bronchiolar epithelium that becomes associated with alveolar gas exchange areas different at 3 months than at 20 months? Does extended exposure, up to essentially a lifetime, show a progressive change with a differing pattern in the degree of tissue reorganization within the central acinus?

The sampling strategy designed for this study allowed us to examine the heterogeneity of the lung's response to ozone within the pulmonary acinus at specified distances from the BADJ. The placement of concentric circles over the geometric center at the first alveolar outpocketing allowed us to divide the isolated tissue systematically into specific 100-μm intervals. This technique provided an unbiased selection of tissues for objective analyses and facilitated the measurement of changes within the alveolar duct as a function of distance. Evaluation of multiple ventilatory units from animals exposed to each ozone concentration permitted us to define in detail the types of changes and remodeling that occur within each tissue compartment forming the alveolar duct or ventilatory unit as oxidant gases proceed deeper into the gas exchange regions of the lung.

Total Epithelial Volume Density

This analysis found significant differences in epithelial volume density between the cranial and caudal sites (Table 2). Based on dosimetry models, one would predict a greater delivered dose to the cranial site and, hence, a greater

response than at the caudal location. This trend was most consistently observed in the parameter X1. For rats exposed either for 3 months or for 20 months, the distance into the ventilatory unit from the BADJ that the epithelial volume density remained at or close to its initial value was not statistically different in either control animals or in those exposed to 0.12 ppm, although it was qualitatively lower at the caudal site than the cranial in the latter exposure group. Following exposure to 1.0 ppm ozone, however, the distance into the ventilatory unit that the volume density remained elevated was 137 μm (3-month exposure) or 257 μm (20-month exposure) at the cranial site, which was significantly further into the ventilatory unit than it was for the control animals. In the caudal site, however, no statistically significant differences were observed. In contrast, the distance into the ventilatory unit at which the lower value of the volume density was observed (X2) was not statistically significantly different between the cranial and caudal sites. The epithelial volume density at 100 μm into the ventilatory unit in both the cranial and caudal sites was significantly elevated compared to control animals following exposure to 1.0 ppm ozone in animals exposed for either 3 or 20 months. Additionally, at the cranial site, the increase following 1.0 ppm ozone for 20 months was significantly greater than at the same exposure for 3 months.

In the 20-month study, intra-animal variability in the fit of individual curves increased after exposure to 1.0 ppm ozone. This increase would suggest that, within an individual animal, there is heterogeneity in ozone response even along a representative ventilatory unit in an identified location. The differences in response were generally qualitative but not statistically significant. The trends for both studies can be seen in Figures 5A, B, and C. As indicated by the standard error bars, there was substantial inter-animal variability. In order to detect statistically significant differences in the trends, larger sample sizes than we used in either study would have been required.

Interstitial Volume Density

When evaluating changes in both epithelial and interstitial volume density, the observed response differs by characteristics of the repiratory tract path (e.g., length, distal volume, branching angles), as illustrated by the significant differences between the cranial and caudal sites. The cranial site is associated with a short path and would be expected to receive a greater dose than would be received at the caudal site, which is associated with a much longer respiratory tract path. Because sites with bronchioles of similar diameters were selected, it is expected that both sites should have similar distal volumes, although that is not known with certainty. Distal volume and path length are the two factors that most influence delivered dose of gases (Mercer et al. 1991b). The site-related differences are much more pronounced in the epithelium than in the interstitium. This effect on the epithelium is also consistent with what is known about ozone. Because ozone is a highly reactive gas, it is likely that most of the damaging interactions take place in the epithelium, and that few ozone molecules reach the interstitium.

ANTIOXIDANT ENZYME LOCALIZATION

Long-term exposure to ozone resulted in a number of changes in the expression of SOD within rat lungs. Cu-Zn SOD decreased in the small airways and in the distal parenchyma, a region of the lung not normally associated with damage from ozone exposure. Cu-Zn SOD has been previously found to be elevated in whole lung homogenates following short-term exposures (Rahman et al. 1991). However, Cu-Zn SOD has been found to be significantly reduced in fetal lungs with respiratory disease (Parizada et al. 1991), which was interpreted to reflect the fetal lung's susceptibility to hyperoxic injury. The current finding of a reduction in Cu-Zn SOD expression diffusely in the lung following long-term ozone exposure is in contrast to the increase in whole lung Cu-Zn SOD described following a short-term exposure (Rahman et al. 1991).

Animals exposed to ozone long-term had a site-specific and cell-specific increase in Mn SOD. Mn SOD was increased in type II epithelial cells located in alveolar duct ridges and adjacent septa up to 400 μm from BADJ. Endotoxin has been shown to cause an increase in Mn SOD but not Cu-Zn SOD and protects against hyperoxia (Tang et al. 1994). Also, intense staining for Mn SOD has been localized in the type II epithelial cells in bronchopulmonary dysplasia, a disease characterized by increased proliferation of type II epithelial cells (Dobashi et al. 1993). Thus, changes in Mn SOD may be more important than changes in Cu-Zn SOD in modulating chronic fibrotic oxidant injury of the lung and proliferative repair processes.

There was no increase in Mn SOD in fibroblasts or in Clara cells. Neither Clara cells found in terminal bronchioles nor Clara cells found in alveolar ducts as a result of bronchiolarized metaplasia after long-term ozone exposure showed an increase in Mn SOD labeling. Bronchiolarized metaplasia of the alveolar ducts is a known result of long-term high-dose (0.5 to 1.0 ppm) exposure to ozone (Barr et al. 1988; Fujinaka et al. 1985; Hiroshima et al. 1989; Pinkerton et al. 1993; Stockstill et al. 1995). A previous study of rats exposed to 1.0 ppm ozone for 20 months found extensive bronchiolarized metaplasia of the alveolar ducts (Stock-

still et al. 1995). The normal type I and type II epithelium lining the alveolar ducts was replaced by cuboidal epithelium composed of ciliated cells, Clara cells, and undifferentiated cuboidal cells (Stockstill et al. 1995). The lack of major cell and tissue changes in some studies on terminal bronchioles following long-term ozone exposure (Barry et al. 1988; Chang et al. 1988b, Stockstill et al. 1995) would seem to indicate an increased tolerance for ozone in the bronchiolar metaplastic tissue, which is similar to tissue found in terminal bronchioles. Other studies have noted some changes in terminal bronchioles exposed to ozone including increased levels of Clara cell secretory protein (Dodge et al. 1994) and an increased mass of nonciliated cells (Plopper et al. 1994a). However, any possible enhanced tolerance of terminal bronchiolar tissue does not involve cell-specific increases in Mn SOD or Cu-Zn SOD. We found that Mn SOD and Cu-Zn SOD were similar in Clara cells located within the alveolar ducts compared to Clara cells in normal bronchiolar tissue after 2 months of exposure to 1.0 ppm ozone. However, other antioxidant enzymes, which were not examined, could be altered by exposure, and thus contribute in yet undefined ways to this tissue's resistance to the oxidant damage from ozone.

A previous investigation of the chronic effects of ozone on alveolar-duct epithelium reported an increase in epithelial thickness, with thickening of type I cells and hyperplasia of type II cells (Chang et al. 1992). Areas in which type I and type II epithelium were maintained in alveolar ducts were found, in addition to areas of bronchiolarized metaplasia after exposure for 20 months to 1.0 ppm ozone (Stockstill et al. 1995). The present study contributes to our understanding of how portions of the alveolar epithelium develop resistance to chronic ozone damage. The alveolar epithelial response seen after 2 months of exposure is similar to that found after 20 months of exposure, and contains a mixed population of epithelial cells with areas made up of Clara, ciliated, and other cuboidal cells as well as areas with type I and type II alveolar epithelial cells (Stockstill et al. 1995). We found a statistically significant increase in the density of Mn SOD in the mitochondria of type II epithelial cells located in the most proximal regions of the alveolar duct walls and septa. Thus, the increased expression of Mn SOD may be associated with type II epithelial cells' becoming more resistant to ozone damage and enabling maintenance of the type I and type II epithelium between areas of bronchiolarized metaplasia in long-term, high-dose ozone exposures.

The site in the lung most affected by ozone exposure is the centriacinar region (Stephens et al. 1974; Chang et al. 1992; Stockstill et al. 1995). The effects of prolonged exposure to ozone in this region include epithelial changes, chronic inflammation, and fibrosis (Chang et al. 1992; Stockstill et al. 1995). Tolerance to ozone exposure in the centriacinar region may involve more than one process. Clara cells are resistant to ozone exposure, and the bronchiolarized metaplasia seen in long-term exposures may be a protective mechanism for the tissue (Stockstill et al. 1995), yet this tolerance does not involve an increase in the antioxidant enzyme Mn SOD. Type II epithelial cells found in the same region as the bronchiolarized Clara cells have increased levels of Mn SOD, suggesting that their tolerance to ozone exposure is associated with an antioxidant increase. An earlier study of the centriacinar region demonstrated a two-fold increase in total SOD activity following a 3-month exposure to ozone, but did not identify which cell types were involved in this increase or the subtype of SOD involved (Plopper et al. 1994b).

CONCLUSIONS

In summary, statistically significant changes were clearly seen in the epithelial, interstitial, and macrophage volume densities of rat lungs following exposure to 1.0 ppm ozone for 3 months as well as for 20 months. Of interest, aging did not affect the anatomical response of rats to ozone during 20 months of exposure, as demonstrated by our calculations of total epithelial and interstitial volume densities after 3 months of exposure not being significantly different from those after 20 months of exposure. No significant effects were noted following exposure to 0.12 ppm ozone. However, the possibility of a significant effect cannot be totally dismissed. Larger sample sizes than we used in these studies would help elucidate whether the trends observed in this study would be strengthened with replication.

The present study demonstrates that ozone-induced increases in total SOD are the result of increases in Mn SOD in type II epithelial cells located along the proximal portion of alveolar duct walls and the adjacent alveolar septa.

ACKOWLEDGMENTS

The authors wish to acknowledge Janice Peake and Courtney Siverson for their technical assistance during the course of this study. The authors also acknowledge the enthusiastic assistance of UC Davis National Science Foundation Young Scholars Tom Castillo, Janice Jim, and Josh Mukhopadhyay in the completion of this work.

REFERENCES

Barr BC, Hyde DM, Plopper CG, Dungworth DL. 1988. Distal airway remodeling in rats chronically exposed to ozone. Am Rev Respir Dis 137:924–938.

Barr BC, Hyde DM, Plopper CG, Dungworth DL. 1990. A comparison of terminal airway remodeling in chronic daily versus episodic ozone exposure. Toxicol Appl Pharmacol 106:384–407.

Barry BE, Miller FJ, Crapo JD. 1985. Effects of inhalation of 0.12 and 0.25 parts per million ozone on the proximal alveolar region of juvenile and adult rats. Lab Invest 53:692–704.

Barry BE, Mercer RR, Miller FJ, Crapo JD. 1988. Effects of inhalation of 0.25 parts per million ozone on the terminal bronchioles of juvenile and adult rats. Exp Lung Res 14:225–245.

Boorman GA, Schwartz LW, Dungworth DL. 1980. Pulmonary effects of prolonged ozone insult in rats: Morphometric evaluation of the central acinus. Lab Invest 43(2):108–115.

Chang L-Y, Slot JW, Geuze HJ, Crapo JD. 1988a. Molecular immunocytochemistry of the CuZn superoxide dismutase in rat hepatocytes. J Cell Biol 107(6):2169–2179.

Chang LY, Mercer RR, Stockstill BL, Miller FJ, Graham FA, Ospital JJ, Crapo JD. 1988b. Effects of low levels of NO_2 on terminal bronchiolar cells and its relative toxicity compared to O_3. Toxicol Appl Pharmacol 96:451–464.

Chang L-Y, Huang Y, Stockstill BL, Graham JA, Grose EC, Ménache MG, Miller FJ, Costa DL, Crapo JD. 1992. Epithelial injury and interstitial fibrosis in the proximal alveolar regions of rats chronically exposed to a simulated pattern of urban ambient ozone. Toxicol Appl Pharmacol 115:241–252.

Dobashi K, Asayama K, Hayashibe H, Munim A, Kawaoi A, Morikawa M, Nakazawa S. 1993. Immunohistochemical study of copper-zinc and manganese superoxide dismutases in the lungs of human fetuses and newborn infants: Developmental profile and alterations in hyaline membrane disease and bronchopulmonary dysplasia. Virchows Arch A Pathol Anat Histol 423:177–184.

Dodge DE, Rucker RB, Pinkerton KE, Haselton CJ, Plopper CG. 1994. Dose-dependent tolerance to ozone. III. Elevation of intracellular Clara cell 10-kDa protein in central acini of rats exposed for 20 months. Toxicol Appl Pharmacol 127:109–123.

Dungworth DL, Cross CE, Gillespie JR, Plopper CG. 1975. The effect of ozone on animals. In: Ozone Chemistry and Technology: A review of the literature, 1961–1974 (Murphy JS, Orr JR, eds.) pp. 29–54. Franklin Institute, Philadelphia, PA.

Fujinaka LE, Hyde DM, Plopper CG, Tyler WS, Dungworth DL, Lollini LO. 1985. Respiratory bronchiolitis following long-term ozone exposure in bonnet monkeys: A morphometric study. Exp Lung Res 8:167–190.

Hiroshima K, Kohno T, Ohwada H, Hayashi Y. 1989. Morphological study of the effects of ozone on rat lung: II. Long-term exposures. Exp Mol Pathol 50:270–280.

Hyde DM, Plopper CG, St. George JA, Harkema JR. 1990. Morphometric cell biology of air space epithelium. In: Electron Microscopy of the Lung (Schraufnagel DE, ed.) pp. 71–120. Marcel Dekker, New York, NY.

Hyde DM, Magliano DJ, Plopper CG. 1992. Morphometric assessment of pulmonary toxicity in the rodent lung. Toxicol Pathol 19:428–446.

Kinnula VL, Yankaskas JR, Chang L-Y, Virtanen I, Linnala A, Crapo JD. 1994. Primary and immortalized (BEAS 2B) human bronchial epithelial cells having significant antioxidative capacity in vivo. Am J Respir Cell Mol Biol 11(5):568–576.

Miller FJ, Overton J, Jasket R, Menzel DB. 1985. A model of the regional uptake of gaseous pollutants in the lung: I. The sensitivity of the uptake of ozone in the human lung to lower respiratory tract secretions and exercise. Toxicol Appl Pharmacol 79:11–27.

Miller FJ, Overton JH, Gerrity TR, Graham RC. 1988. Interspecies dosimetry of reactive gases. In: Inhalation Toxicology (Mohr U, Dungworth D, Kimmerle G, Lewkowski J, McClellan R, Stöber W, eds.) pp. 139–155. Springer-Verlag, New York, NY.

Nikula KJ, Wilson DW, Giri S, Plopper CG, Dungworth DL. 1988. The response of rat tracheal epithelium to ozone exposure: Injury, adaptation, and repair. Am J Pathol 131:373–384.

Oprins A, Geuze HJ, Slot JW. 1994. Cryosubstitution dehydration of aldehyde-fixed tissue: A favorable approach to quantitative immunocytochemistry. J Histochem Cytochem 42:497–503.

Overton JH, Graham RC, Miller FJ. 1987. A model of the regional uptake of gaseous pollutants in the lung: II. The

sensitivity of ozone uptake in laboratory animal lungs to anatomical and ventilatory parameters. Toxicol Appl Pharmacol 88:418–432.

Overton JH, Barnett AE, Graham RC. 1989. Significances of the variability of tracheobronchial airway paths and their air flow rates to dosimetry model prodictions of the absorption of gases. In: Extrapolation of Dosimetric Relationships for Inhaled Particles and Gases (Crapo JD, Duke University Center for Extrapolation Modeling, eds.) pp. 273–291. Academic Press, New York, NY.

Patra AL, Gooya A, Ménache M. 1986. A morphometric comparison of the nasopharyngeal airway of laboratory animals and humans. Anat Rec 215:42–50.

Parizada B, Werber MM, Nimrod A. 1991. Protective effects of human recombinant MnSOD in adjuvant arthritis and bleomycin-induced lung fibrosis. Free Radic Res Commun 15(5):297–301.

Phalen RF, Yeh HC, Schum GM, Raabe OG. 1978. Application of an idealized model to morphometry of the mammalian tracheobronchial tree. Anat Rec 190:167–176.

Phalen RF, Oldham MJ. 1983. Tracheobronchial airway structure as revealed by casting techniques. Am Rev Respir Dis 128:51–53.

Pinkerton KE, Barry BE, O'Neil JJ, Raub JA, Pratt PC, Crapo JD. 1982. Morphologic changes in the lung during the lifespan of Fischer 344 rats. Am J Anat 164:155–174.

Pinkerton KE, Dodge DE, Cederdahl-Demmler J, Wong VJ, Peake J, Haselton CJ, Mellick PW, Singh G, Plopper CG. 1993. Differentiated bronchiolar epithelium in alveolar ducts of rats exposed to ozone for 20 months. Am J Pathol 142:947–956.

Pinkerton KE, Ménache MG, Plopper CG. 1995. Consequences of Prolonged Inhalation of Ozone on F344/N Rats: Collaborative Studies, Part IX, Changes in the Tracheobronchial Epithelium, Pulmonary Acinus, and Lung Antioxidant Enzyme Activity. Research Report Number 65. Health Effects Institute, Cambridge, MA.

Plopper CG. 1990. Structural methods for studying bronchiolar epithelial cells. In: Models of Lung Disease: Microscopy and Structural Methods (Gil J, ed.) pp. 537–559. Marcel Dekker, New York, NY.

Plopper CG, Macklin J, Nishio SJ, Hyde DM, Buckpitt AR. 1992. Relationship of cytochrome P450 activity to Clara cell cytotoxicity: III. Morphometric comparison of changes in the epithelial populations of terminal bronchioles and lobar bronchi in mice, hamsters, and rats after parenteral administration of naphthalene. Lab Invest 67:553–565.

Plopper CG, Chu F-P, Haselton CJ, Peake J, Wu J, Pinkerton KE. 1994. Dose-dependent tolerance to ozone: I. Tracheobronchial epithelial reorganization in rats after 20 months of exposure. Am J Pathol 144:404–420.

Plopper CG, Duan X, Buckpitt AR, Pinkerton KE. 1994. Dose-dependent tolerance to ozone: IV. Site-specific elevation in antioxidant enzymes in the lungs of rats exposed for 90 days or 20 months. Toxicol Appl Pharmacol 127:124–131.

Project Staff. 1995. Consequences of Prolonged Inhalation of Ozone on F344/N Rats: Collaborative Studies, Part VI, Background and Project Design. Research Report Number 65. Health Effects Institute, Cambridge, MA.

Raabe OG, Yeh HC, Schum GM, Phalen RF. 1976. Tracheobronchial Geometry: Human, Dog, Rat, Hamster. Technical Report LF-53. Lovelace Foundation for Medical Education and Research, Albuquerque, NM.

Rahman IU, Clerch LB, Massaro D. 1991. Rat lung antioxidant enzyme induction by ozone. Am J Physiol 260:L412–L418.

Slot JW, Geuze HJ. 1984. Gold markers for single and double immunolabeling of ultrathin cryosections. In: Immunoblotting for Electron Microscopy (Polak JM, Varndell IM, eds.) pp. 129–142. Elsevier Science Publishing Co., New York, NY.

Slot JW, Geuze HJ. 1985. A new method of preparing gold probes for multiple-labeling cytochemistry. Eur J Cell Biol 38:87–93.

Slot JW, Geuze HJ, Freeman BA, Crapo JD. 1986. Intracellular localization of the copper-zinc and manganese superoxide dismutases in rat liver parenchyma cells. Lab Invest 55(3):363–371.

Stephens RJ, Sloan MF, Evans MJ, Freeman G. 1974. Early response of lung to low levels of ozone. Am J Pathol 74:31–58.

Stockstill BL, Chang L-Y, Ménache MG, Mellick PW, Mercer RR, Crapo JD. 1995. Bronchiolarized metaplasia and interstitial fibrosis in rat lungs chronically exposed to high ambient levels of ozone. Toxicol Appl Pharmacol 134:251–263.

Tang G, Berg JT, White JE, Lumb PD, Lee CY, Tsan MF. 1994. Protection against oxygen toxicity by tracheal insufflation of endotoxin: Role of Mn SOD and alveolar macrophages. Am J Physiol 266(10): L38–L45.

ABOUT THE AUTHORS

Kent E. Pinkerton is an Associate Professor in Residence in the Department of Anatomy, Physiology, and Cell Biology in the School of Veterinary Medicine, University of California, Davis. He completed his undergraduate education at Brigham Young University in 1974 and received the M.S. and Ph.D. degrees in pathology from Duke University in 1978 and 1982, respectively. His primary research interests are in respiratory cell biology and environmental air pollutants.

Barbara L. Weller is a Research Associate in the Department of Medicine, School of Medicine, University of California, Davis. She completed her undergraduate education at North Carolina State University and received the Ph.D. degree in pathology from Duke University in 1995. Her primary research interest is antioxidant-induced tolerance in epithelial adaptation to long-term ozone exposure.

Margaret G. Ménache is currently a biostatistician at Lovelace Respiratory Research Institute, Albuquerque, NM. She holds Masters degrees in economics and biostatistics. At the time of this research, she was completing her Ph.D. degree in the School of the Environment at Duke University. Her research interest is modeling for gas and particle dosimetry in the human respiratory tract.

Charles G. Plopper is a Professor in the Department of Anatomy, Physiology, and Cell Biology in the School of Veterinary Medicine, University of California, Davis. He completed his undergraduate education in 1967 and his Ph.D. degree in anatomy in 1972, both at the University of California, Davis. His primary research interests are in respiratory cell biology and environmental air pollutants.

PUBLICATIONS RESULTING FROM THIS RESEARCH

Weller BL, Crapo JD, Slot J, Posthuma G, Plopper CG, Pinkerton KE. 1997. Site- and cell-specific alteration of lung copper/zinc and manganese superoxide dismutases by chronic ozone exposure. Am J Respir Cell Mol Biol 17:552–560.

ABBREVIATIONS

ANOVA	analysis of variance
BADJ	bronchiole-alveolar duct junction
BSA	bovine serum albumin
Cu-Zn SOD	copper-zinc superoxide dismutase
MANOVA	multivariate analysis of variance
Mn SOD	manganese superoxide dismutase
mOsm	milliosmolal
mPa	milliPascal
NTP	National Toxicology Program
PBS	phosphate-buffered saline
ppm	parts per million
SOD	superoxide dismutase

INTRODUCTION

In 1987, the National Toxicology Program (NTP)* and the Health Effects Institute initiated a collaborative project to determine whether long-term exposure to ozone produces changes in the respiratory tract of rats. The NTP exposed rats and mice to ozone alone for 24 or 30 months or to ozone plus the lung carcinogen 4-(*N*-methyl-*N*-nitrosamino)-1-(3-pyridyl)-1-butanone for 24 months (National Toxicology Program 1995). The NTP studies focused on carcinogenesis. The HEI-funded investigators analyzed changes in the structure, biochemistry, and function of the respiratory tract of F344/N rats exposed for 20 months to clean air (0 ppm ozone) or to 0.12, 0.5, or 1.0 ppm ozone. The results of these studies, including an integrative summary of nine individual studies and a description of the project design, were published as Parts I through XII of HEI Research Report Number 65.

As part of the NTP/HEI collaboration, Dr. Kent Pinkerton and colleagues provided a detailed analysis of ozone's changes on the microscopic structure and antioxidant enzyme activities in rat lungs and airways (Pinkerton et al. 1995). However, because the number of rats was limited, analyses were performed only after 20 months of exposure. Thus, it was not known when these changes took place or if aging during the exposure period modified the animals' response to ozone. To address these questions, Dr. Pinkerton proposed additional research to examine the same endpoints in rats exposed to ozone for 2 or 3 months. Because this was an opportunity to obtain information on the time course of ozone-induced changes, the HEI Health Research Committee funded one year of additional research that began in May 1995.† The following Commentary on the Investigators' Report is intended to aid the sponsors of HEI and the public by highlighting both the strengths and limitations of the study and by placing the Investigators' Report into scientific and regulatory perspective.

SCIENTIFIC BACKGROUND

Here we present a brief overview of selected aspects of ozone's effects on the airways. The Health Review Committee's Commentary on Parts VIII and IX of Research Report Number 65 (which contains the independent studies by Dr. Ling-Yi Chang and colleagues and Dr. Pinkerton and coworkers) provides a more detailed discussion.

In general, the tracheobronchial conducting airways (trachea, bronchi, and bronchioles) do not show histopathologic changes after exposure to ozone concentrations as high as 1 ppm. This is due to their small surface area and the relatively thick mucous layer that protects the underlying epithelium. Mathematical models predict that the tissue dose of ozone increases appreciably at the centriacinar region (the junction of the conducting airways and the gas exchange region). In this region, the area of lung surface exposed to ozone increases and the mucous layer thins (Miller et al. 1985; Overton and Graham 1989; Grotberg et al. 1990). The primary site of tissue damage in animals exposed to ozone is at the acinar entrance, the bronchoalveolar duct junction (BADJ) (Stephens et al. 1974; Mellick et al. 1977). The major change in this region in rats exposed to ozone for 2 to 3 months is bronchiolarization of the centriacinar alveolar ducts (Boorman et al. 1980; Barr et al. 1988). As a result, the thinner, ozone-sensitive cells normally lining the alveolar ducts in the centriacinar region are replaced by thicker, ozone-resistant cells that are more characteristic of small bronchioles. As bronchiolar epithelium extends into the alveolar duct, respiratory bronchioles are formed in species that normally do not have them (Boorman et al. 1980; Moore and Schwartz 1981) and the volume of the respiratory bronchioles increases (a condition called respiratory bronchiolitis) in animals that do have them (Fujinaka et al. 1985; Tyler et al. 1988).

Ozone exposure can injure the lungs directly by damaging cell membrane components, or indirectly by causing the release of oxidants from inflammatory cells recruited to the lungs by ozone inhalation. Protection against oxidant injury is provided by antioxidant enzymes (superoxide dismutases [SOD], glutathione peroxidase, glutathione *S*-transferases, glutathione reductase) that inactivate the oxidants either directly, or via nonenzymatic reductants such as reduced glutathione. Lung tissues respond to short-term

* A list of abbreviations appears at the end of the Investigators' Report for your reference.

† Dr. Kent E. Pinkerton's one-year study, *Consequences of Prolonged Inhalation of Ozone on F344/N Rats: Collaborative Studies, Part XIII. A Comparison of Changes in the Tracheobronchial Epithelium and Pulmonary Acinus in Male Rats at 3 and 20 Months*, began in May 1995 and had total expenditures of $128,065. The Investigators' Report from Pinkerton and colleagues was received for review in November 1996. A revised report, received in October 1997, was accepted for publication at that time. During the review process, the HEI Review Committee and the investigators had the opportunity to exchange comments and to clarify issues in the Investigators' Report and in the Review Committee's Commentary.

exposure to ozone by increasing antioxidant enzyme activities (Clark et al. 1978; Rietjens et al. 1985; Heng et al. 1987; Elsayed et al. 1988; Ichinose and Sagai 1989; Van Bree et al. 1992). In their NTP/HEI study, Pinkerton and coworkers (1995) reported that bronchiolarization of the alveolar ducts occurred, and that total SOD activity and glutathione peroxidase activity increased in the bronchiole-centriacinar region in rats exposed to 0.5 or 1.0 ppm ozone for 20 months.

Because the bronchiolar epithelium resisted injury by ozone and the level of antioxidant enzymes increased in the bronchiole-centriacinar region, Pinkerton and colleagues (1995) hypothesized that these changes occur early in the exposure period and protect the centriacinar region from ozone-induced injury. To support their hypothesis, it was necessary for Pinkerton and coworkers to determine when the biochemical and cellular changes they observed after 20 months of ozone exposure occurred. If changes occurred early and were stable over 20 months, they might be responsible for the protective effects proposed by the investigators. However, if the early changes decreased or worsened over 20 months, a putative protective effect might not occur.

OBJECTIVES

The overall objective of Pinkerton's present study was to determine ozone's effects on the structure and antioxidant enzyme activities of target and nontarget sites of the tracheobronchial tree and pulmonary acini after 2 or 3 months of exposure and to compare these results with those seen after 20 months of exposure.

The specific aims were to:

1. Determine if the bronchiolar-centriacinar remodeling seen after 20 months of ozone exposure was present after a 2- or 3-month exposure and determine the extent of remodeling at the earlier time points;
2. Assess the extent to which the changes seen after the 20-month exposure represented aging rather than a response to ozone;
3. Determine the changes in copper-zinc (Cu-Zn) SOD and manganese (Mn) SOD expression in the cytosol and mitochondria, respectively, after 2 or 3 months of exposure to ozone; and
4. Determine whether the effects of aging on the tracheobronchial tree and pulmonary acini override the effects of exposure to 0.12 ppm ozone (the National Ambient Air Quality Standard in effect when the study was performed, which was not to be exceeded for more than one hour, once per year).

TECHNICAL EVALUATION

METHODS AND STUDY DESIGN

The study design and methods conformed to those used for the 20-month NTP/HEI study (Pinkerton et al. 1995) with the following exceptions: (1) rats were exposed to clean air or ozone at the California Regional Primate Research Center of the University of California, Davis, rather than at Battelle Pacific Northwest Laboratories in Richland, WA; (2) only male rats were studied (because they appeared to be more sensitive to ozone than females in Pinkerton's 20-month exposure study); (3) ozone exposure levels were 0, 0.12, and 1.0 ppm (the NTP/HEI study included a 0.5-ppm concentration); (4) rats were killed after either 2 or 3 months of exposure; and (5) animals were killed 24 hours after exposure ceased, rather than one week after exposure as in the 20-month study.

The study was performed with rigorous attention to the details of ozone dosimetry and morphometric and immunohistologic analyses. A particular strength of the experimental design was the tissue sampling technique, which ensured that comparable regions of the lung were studied in each animal. The investigators used microdissection techniques to examine sites within the tracheobronchial tree and pulmonary acini by morphometric and immunohistochemical analyses. Morphometric methods were used to determine ozone-induced changes in epithelial thickness and the volume fraction of various cell types (epithelial cells, interstitial cells, and macrophages) and anatomic compartments such as capillary lumina. An important aspect of these analyses was the proper location of the BADJ, which was designated as the site of the first alveolar outpocketing. Pinkerton and colleagues studied changes at BADJ sites that arose from short (cranial) or long (caudal) tracheobronchial paths to the acinar region. They used immunohistologic approaches with both light and electron microscopy to localize and quantify the levels of Cu-Zn SOD and Mn SOD.

For data analysis, the investigators used a series of statistical procedures, established in their earlier study (Pinkerton et al. 1995), that deal effectively with multivariate data. One method consisted of classifying dependent or outcome variables into sets related to various hypotheses. As a first step, these sets underwent appropriate multivariate analysis of variance (MANOVA) to establish if significance existed. These analyses examined the dependent variables jointly such as ozone dose, length of exposure (3 or 20 months) and their interactions. If statistical significance ($p < 0.05$) by the Hotelling-Lawley trace test was established by the multivariate analyses, each dependent variable was

subjected to a second analysis by a two-way analysis of variance (ANOVA). A third step consisted of separate *t* tests performed on variables identified as significant in the second step by the ANOVA *F* test. The investigators stopped their analyses at any step that did not show statistical significance. They also developed variations of these procedures that incorporated repeated measures analysis. In some cases, they first determined summary statistics, such as slopes, for later use in their analyses. Because they used this step-down procedure, the investigators did not need to adjust for multiple comparisons.

RESULTS AND INTERPRETATIONS

The principal findings were the following:

1. The lungs of male F344/N rats exposed to 0.12 ppm ozone for 3 months did not show any structural changes compared with control rats that breathed clean air. This is consistent with the findings of the 20-month exposure study (Pinkerton et al. 1995). Although the results of both studies indicate that exposure to 0.12 ppm ozone does not produce structural changes in healthy animal lungs, they do not exclude the possibility that prolonged exposure to this, or even lower, ozone levels may alter lung responses to other agents, such as viruses, nor do they exclude the possibility that prolonged exposure may cause deleterious effects to humans with lung disease.
2. Rats exposed to 1.0 ppm ozone for 2 or 3 months showed morphometric changes that were similar to those seen after 20 months. For example, bronchiolarized metaplasia in alveolar ducts had occurred after 2 months of exposure. This change was confined to the alveoli within 200 μm of a terminal bronchiole. Also in agreement with the findings of the 20-month study was the observation that the largest effects of 1.0 ppm ozone were at BADJs in cranial sites. As the authors point out, because cranial BADJs are associated with a shorter respiratory tract path than BADJs at caudal sites, they would be expected to receive a greater dose of ozone. Thus, ozone's effects decreased as the path length leading to the BADJ increased.
3. The effect of exposure to 1.0 ppm ozone was greater in the epithelium than in the interstitium, which is consistent with ozone being most reactive with the first tissue it encounters.
4. Exposure to 1.0 ppm ozone for 2 months had no effect on the expression of Cu-Zn SOD in any cell type in the terminal bronchioles or the alveolar ducts. In contrast, exposure to this ozone concentration increased the expression of Mn SOD in the mitochondria of type II alveolar epithelial cells located within 400 μm of the BADJ. Mn SOD expression in Clara cells in the BADJ was unaffected by exposure to 1.0 ppm ozone. These findings suggest that upregulation of Mn SOD by alveolar type II cells confers resistance to ozone. In their earlier study (Pinkerton et al. 1995), the investigators reported an increase in total SOD activity in the BADJ after exposure to 1.0 ppm ozone. The results of the present study suggest that the increased expression of mitochondrial Mn SOD in type II cells was responsible for this change.

The investigators propose that Mn SOD in Clara cells plays a lesser role in protection against ozone because its expression was not enhanced. However, the basal level of Mn SOD was higher in Clara cells than in type II cells and the investigators consider Clara cells to be relatively resistant to ozone. Thus, it is possible that the basal level of Mn SOD in Clara cells is sufficient to protect them. In addition to induction of the enzyme in type II cells, the increase in total SOD activity in the BADJ region seen in their NTP/HEI study could have been caused, in part, by bronchiolar metaplasia in alveolar ducts that replaced epithelial cells containing low levels of Mn SOD with Clara cells containing high levels of Mn SOD.

In summary, this study shows a heterogeneous response of the alveolar duct to ozone exposure that depends on the distance from the BADJ. The results of this intermediate-term exposure agree with the results of the 20-month exposure study and indicate that the morphologic changes and increased antioxidant enzyme levels present after 20 months of exposure to ozone occur early and are stable. The similar changes at the two time points also indicate that aging did not affect the rat lung's response to ozone. The morphologic changes and increased antioxidant enzyme levels seen after 2 or 3 months of exposure to 1.0 ppm ozone suggest that these responses may have protected the rat lung from further injury during continued exposure to ozone. However, these responses to ozone may not necessarily be beneficial to lung health in general because the centriacinar remodeling represents a change from normal anatomy. We do not know if these structural changes in the small airways reverse over time if ozone exposure decreases or, if not, what the long-term consequences of the altered lung anatomy may be.

IMPLICATIONS FOR FUTURE RESEARCH

Increased expression of Mn SOD in alveolar epithelial type II cells may represent an important protective response to ozone exposure. Further evidence that intracellular antioxidants protect against ozone damage may encourage

researchers to explore therapeutic strategies using exogenous addition of antioxidants or upregulation of antioxidant enzyme levels by lung cells. The results of two investigations suggest that this may be a worthwhile area to pursue. In one study, ozone-induced bronchiolar inflammation in rats was prevented by adding the antioxidant taurine to the rats' drinking water for ten successive days prior to ozone inhalation (Schuller-Levis et al. 1995). In another study, administration of Mn SOD (but not Cu-Zn SOD) inhibited bleomycin-induced lung fibrosis in rats. The fibrotic action of bleomycin is thought to be mediated in part by oxygen free radicals (Parizada et al. 1991).

CONCLUSIONS

In an earlier study that was part of the NTP/HEI Collaborative Ozone Project, Pinkerton and colleagues (1995) reported structural and biochemical changes in the respiratory tract tissue of male and female F344/N rats exposed to 0.5 or 1.0 ppm ozone for 20 months. However, conclusions regarding when these changes occurred or how they evolved could not be drawn because information on earlier time points was not collected.

In their present study, the investigators exposed male F344/N rats to 0, 0.12, or 1.0 ppm ozone for either 2 or 3 months and compared their observations with those found after 20 months of exposure. The results of this study confirm and extend their original findings. The lungs of male rats exposed to 0.12 ppm ozone for 3 months did not show any structural changes compared with control rats that breathed clean air. The greatest effects of exposure to 1.0 ppm ozone were seen in the centriacinar region close to the BADJ, a site that mathematical models predict is a target area for inhaled ozone. Morphometric changes in the centriacinar region (epithelial thickening, bronchiolarization of the alveolar duct) were seen after 2 or 3 months of exposure to 1.0 ppm ozone, and the degree of these changes was similar to that seen after 20 months of exposure to 1.0 ppm ozone. Thus, the ozone-induced changes do not appear to have been affected by aging. These changes alter the anatomy of the centriacinar region and it is not known if this is detrimental to lung health over the long term. The increased centriacinar antioxidant enzyme activity reported in the investigators' NTP/HEI study after exposure to 1.0 ppm ozone for 20 months could be accounted for by an increase in Mn SOD in type II alveolar epithelial cells close to the BADJ after 2 or 3 months of exposure to 1.0 ppm ozone. Taken together, the results indicate that the cellular and antioxidant enzyme changes in response to long-term exposure to ozone occur early and are stable. Accordingly, the early responses to ozone may represent changes that protect the rat lungs during continued exposure to ozone.

ACKNOWLEDGMENTS

The Health Review Committee would like to thank the ad hoc reviewers for their help in evaluating the scientific merit of the Investigators' Report. The Committee is also grateful to Dr. Bernard Jacobson for his assistance in preparing its Commentary, and to Virgi Hepner, Valerie Kelleher, Malti Sharma, and Mary Stilwell for their roles in publishing this report.

REFERENCES

Barr BC, Hyde DM, Plopper CG, Dungworth DL. 1988. Distal airways remodeling in rats chronically exposed to ozone. Am Rev Respir Dis 137:924–938.

Boorman GA, Schwartz LW, Dungworth DL. 1980. Pulmonary effects of prolonged ozone insult in rats: Morphometric evaluation of the central acinus. Lab Invest 43:108–115.

Clark K, Posin C, Buckley R. 1978. Biochemical response of squirrel monkeys to ozone. J Toxicol Environ Health 4:741–753.

Elsayed NM, Kass R, Mustafa MG, Hacker AD, Ospital JJ, Chow CK, Cross CE. 1988. Effect of dietary vitamin E level on the biochemical response of rat lung to ozone inhalation. Drug Nutr Interact 5:373–386.

Fujinaka LE, Hyde DM, Plopper CG, Tyler WS, Dungworth DL, Lollini LO. 1985. Respiratory bronchiolitis following long-term ozone exposure in bonnet monkeys: A morphometric study. Exp Lung Res 8:167–190.

Grotberg JB, Sheth BV, Mockros LF. 1990. An analysis of pollutant gas transport and absorption in pulmonary airways. J Biomed Eng 112:168–176.

Heng H, Rucker RB, Crotty J, Dubick MA. 1987. The effects of ozone on lung, heart, and liver superoxide dismutase and glutathione peroxidase activities in the protein-deficient rat. Toxicol Lett 38:225–237.

Ichinose T, Sagai M. 1989. Biochemical effects of combined gases of nitrogen dioxide and ozone: III. Synergistic effects on lipid peroxidation and antioxidative protective systems in the lungs of rats and guinea pigs. Toxicology 59:259–270.

Mellick PW, Dungworth DL, Schwartz LW, Tyler WS. 1977. Short term morphologic effects of high ambient levels of ozone on the lungs of rhesus monkeys. Lab Invest 36:82–90.

Miller FJ, Overton JH Jr, Jaskot RH, Manzel DB. 1985. A model of the regional uptake of gaseous pollutants in the lung: I. The sensitivity of the uptake of ozone in the human lung to lower respiratory tract secretions and exercise. Toxicol Appl Pharmacol 79:11–27.

Moore PF, Schwartz LW. 1981. Morphologic effects of prolonged exposure to ozone and sulfuric acid aerosol on the rat lung. Exp Mol Pathol 35:108–123.

National Toxicology Program. 1995. Toxicology and Carcinogenesis Studies of Ozone and Ozone/NNK in Fischer-344/N Rats and B6C3F$_1$ Mice. NTP Technical Report No. 400. NIH Publication No. 93-3371. U.S. Department of Health and Human Services, National Toxicology Program Information Office, Research Triangle Park, NC.

Overton JH, Graham RC. 1989. Prediction of ozone absorption in humans from newborn to adult. Health Phys (Suppl 1) 57:29–36.

Parizada B, Werber MM, Nimrod A. 1991. Protective effects of human recombinant MnSOD in adjuvant arthritis and bleomycin-induced lung fibrosis. Free Radic Res Commun 15:297–301.

Pinkerton KE, Ménache MG, Plopper CG. 1995. Consequences of Prolonged Inhalation of Ozone on F344/N Rats: Collaborative Studies. Part IX: Changes in the Tracheobronchial Epithelium, Pulmonary Acinus, and Lung Antioxidant Enzyme Activity. Research Report Number 65. Health Effects Institute, Cambridge, MA.

Rietjens IU, van Bree L, Marra M, Poelen MCM, Rombout PJA, Alink GM. 1985. Glutathione pathway enzyme activities and the ozone sensitivity of lung cell populations derived from ozone exposed rats. Toxicology 37:205–214.

Schuller-Levis GB, Gordon RE, Park E, Pendino KJ, Laskin DL. 1995. Taurine protects rat bronchioles from acute ozone-induced lung inflammation and hyperplasia. Exp Lung Res 21:877–888.

Stephens RJ, Sloan MF, Evans MJ, Freeman G. 1974. Early response of lung to low levels of ozone. Am J Pathol 74:31–58.

Tyler WS, Tyler NK, Last JA, Gillespie MJ, Barstow TJ. 1988. Comparison of daily and seasonal exposures of young monkeys to ozone. Toxicology 50:131–144.

van Bree L, Marra M, Rombout PJA. 1992. Differences in pulmonary biochemical and inflammatory responses of rats and guinea pigs resulting from daytime or nighttime, single and repeated exposure to ozone. Toxicol Appl Pharmacol 116:209–216.

RELATED HEI PUBLICATIONS: ANIMAL REPONSES TO OZONE

Report No.	Title	Principal Investigator	Publication Date
Research Reports			
38	Synergistic Effects of Air Pollutants: Ozone Plus a Respirable Aerosol	J.A. Last	1991
44	Leukocyte-Mediated Epithelial Injury in Ozone-Exposed Rat Lung	K. Donaldson	1991
45	The Effects of Exercise on Dose and Dose Distribution of Inhaled Automotive Pollutants	M.T. Kleinman	1991
48	Effects of Ozone on Airway Epithelial Permeability and Ion Transport	P.A. Bromberg	1991
50	The Role of Ozone in Tracheal Cell Transformation	D.G. Thomassen	1992
60	Failure of Ozone and Nitrogen Dioxide to Enhance Lung Tumor Development in Hamsters	H. Witschi	1993
65	Consequences of Prolonged Inhalation of Ozone on F344/N Rats: Collaborative Studies		
	Part I: Content and Cross-Linking of Lung Collagen	J.A. Last	1994
	Part II: Mechanical Properties, Responses to Bronchoactive Stimuli, and Eicosnaoid Release in Isolated Large and Small Airways	J.L. Szarek	1994
	Part III: Effects on Complex Carbohydrates of Lung Connective Tissue	B. Radhakrishnamurthy	1994
	Part IV: Effects on Expression of Extracellular Matrix Genes	W.C. Parks	1994
	Part V: Effects on Pulmonary Function	J.R. Harkema	1994
	Part VI: Background and Study Design	Project Staff	1995
	Part VII: Effects on the Nasal Mucociliary Apparatus	J.R. Harkema	1994
	Part VIII: Morphometric Analysis of Structural Alterations in Alveolar Regions	L.Y. Chang	1995
	Part IX: Changes in the Tracheobronchial Epithelium, Pulmonary Acinus, and Lung Antioxidant Enzyme Activity	K.E. Pinkerson	1995
	Part X: Robust Composite Scores Based on Median Polish Analysis	P.J. Catalano	1995
	Part XI: Integrative Summary	The Collaborative Ozone Project Group	1995
	Part XII: Atrophy of Bone in Nasal Turbinates	J.R. Harkema	1997
HEI Communication Number 1			
	New Methods of Ozone Toxicology: Abstracts of Six Pilot Studies	L-Y.L. Chang R.A. Floyd W.C. Parks K.E. Pinkerton D.A. Uchida R. Vincent	1992

Copies of these reports can be obtained by writing or calling the Health Effects Institute, 955 Massachusetts Avenue, Cambridge, MA 02139. Phone (617) 876-6700 FAX (617) 876-6709 E-mail pubs@healtheffects.org http://www.healtheffects.org

HEI

The Board of Directors

Archibald Cox *Chairman*
Carl M. Loeb University Professor (Emeritus), Harvard Law School

Douglas Costle
Chairman of the Board and Distinguished Senior Fellow, Institute for Sustainable Communities

Alice Huang
Senior Councilor for External Relations, California Institute of Technology

Donald Kennedy
President (Emeritus) and Bing Professor of Biological Sciences, Stanford University

Susan B. King
Fellow, Sanford Institute of Public Policy, Duke University

Richard B. Stewart
Professor, New York University School of Law

Robert M. White
President (Emeritus), National Academy of Engineering, and Senior Fellow, University Corporation for Atmospheric Research

Health Research Committee

Bernard D. Goldstein *Chairman*
Director, Environmental and Occupational Health Sciences Institute

Glen R. Cass
Professor of Environmental Engineering and Mechanical Engineering, California Institute of Technology

Seymour J. Garte
Professor, Department of Environmental Medicine, New York University Medical Center

Rogene Henderson
Senior Scientist, Lovelace Respiratory Research Institute

Meryl H. Karol
Professor of Environmental and Occupational Health, University of Pittsburgh Graduate School of Public Health

Stephen I. Rennard
Larson Professor, Pulmonary and Critical Care Medicine Section, Department of Internal Medicine, University of Nebraska Medical Center

Jonathan M. Samet
Professor and Chairman, Department of Epidemiology, School of Hygiene and Public Health, Johns Hopkins University

Robert F. Sawyer
Class of 1935 Professor of Energy (Emeritus), Professor of the Graduate School, University of California at Berkeley

Frank E. Speizer
Edward H. Kass Professor of Medicine, Channing Laboratory, Harvard Medical School, Department of Medicine, Brigham and Women's Hospital

Gerald van Belle
Chairman, Department of Environmental Health, School of Public Health and Community Medicine, University of Washington

Health Review Committee

Daniel C. Tosteson *Chairman*
Professor of Cell Biology, Dean Emeritus, Harvard Medical School

John C. Bailar III
Chair, Department of Health Studies, Biological Sciences Division, University of Chicago

A. Sonia Buist
Professor of Medicine and Physiology, Oregon Health Sciences University

Ralph D'Agostino
Professor of Mathematics/Statistics and Public Health, Boston University

Thomas W. Kensler
Professor, Division of Toxicological Sciences, Department of Environmental Sciences, Johns Hopkins University

Donald J. Reed
Distinguished Professor of Biochemistry, Department of Biochemistry and Biophysics, and Environmental Health Sciences Center, Oregon State University

David J. Riley
Professor of Medicine, University of Medicine and Dentistry of New Jersey–Robert Wood Johnson Medical School

Robert M. Senior
Dorothy R. and Hubert C. Moog Professor of Pulmonary Diseases in Medicine, Washington University School of Medicine

Officers and Staff

Daniel S. Greenbaum *President*
Richard M. Cooper *Corporate Secretary*
Howard E. Garsh *Director of Finance and Administration*
Kathleen M. Nauss *Director for Scientific Review and Evaluation*
Robert M. O'Keefe *Director of Program Strategy*
Jane Warren *Director of Research*
Aaron J. Cohen *Senior Scientist*
Maria G. Costantini *Senior Scientist*
Debra A. Kaden *Senior Scientist*
Alison Geyh *Staff Scientist*
Bernard Jacobson *Staff Scientist*
Martha E. Richmond *Staff Scientist*
Geoffrey H. Sunshine *Staff Scientist*
Gail V. Allosso *Senior Administrative Assistant*
Quinette Halley *Administrative Assistant*
L. Virgi Hepner *Managing Editor*
Valerie Kelleher *Publications Production Coordinator*
Francine Marmenout *Administrative Assistant*
Teresina McGuire *Accounting Assistant*
Beverly Morse *Receptionist*
Jacqueline C. Rutledge *Controller*
Malti Sharma *Publications Assistant*
Mary L. Stilwell *Administrative Assistant*

HEI HEALTH EFFECTS INSTITUTE 955 Massachusetts Avenue, Cambridge, MA 02139 (617) 876-6700

Research Report Number 65

June 1998